A robotic honeycomb for interaction with a honeybee colony

Rafael Barmak[1†] and Martin Stefanec[2†], Daniel N. Hofstadler[2], Louis Piotet[1], Stefan Schönwetter-Fuchs-Schistek[2], Francesco Mondada[1], Thomas Schmickl[2], Rob Mills[1]*

[1]Mobile Robotic Systems Group, École Polytechnique Fédérale de Lausanne, Lausanne, Switzerland.
[2]Artificial Life Lab, Department of Zoology, Institute of Biology, University of Graz, Graz, Austria.

*Corresponding author. Email: rob.mills@epfl.ch. †These authors contributed equally to this work.

Title: A robotic honeycomb for interaction with a honeybee colony

Authors:

Rafael Barmak[1†] and Martin Stefanec[2†], Daniel N. Hofstadler[2], Louis Piotet[1], Stefan Schönwetter-Fuchs-Schistek[2], Francesco Mondada[1], Thomas Schmickl[2], Rob Mills[1]*

Affiliations:

[1]Mobile Robotic Systems Group, École Polytechnique Fédérale de Lausanne, Lausanne, Switzerland.

[2]Artificial Life Lab, Department of Zoology, Institute of Biology, University of Graz, Graz, Austria.

*Corresponding author. Email: rob.mills@epfl.ch. †These authors contributed equally to this work.

Abstract:

Robotic technologies have shown the capability to interact with living organisms and even to form integrated mixed societies comprised of living and artificial agents. Bio-compatible robots, incorporating sensing and actuation capable of generating and responding to relevant stimuli, can be a tool to study collective behaviors previously unattainable with traditional techniques. To investigate collective behaviors of the western honeybee (*Apis mellifera*), we designed a robotic system capable of observing and modulating the bee cluster using an array of thermal sensors and actuators. We initially integrated the system into a beehive populated with approximately 4,000 bees for several months. The robotic system was able to observe the colony by continuously collecting spatio-temporal thermal profiles of the winter cluster. Furthermore, we found that our robotic device reliably modulated the superorganism's response to dynamic thermal stimulation, influencing its spatiotemporal re-organization. In addition, after identifying the thermal collapse of a colony, we used the robotic system in a "life-support" mode via its thermal actuators. Ultimately, we demonstrated a robotic device capable of autonomous closed-loop interaction with a cluster comprising thousands of individual bees. Such biohybrid societies open the door to investigation of collective behaviors that necessitate observing and interacting with the animals within a complete social context, as well as for potential applications in augmenting the survivability of these pollinators crucial to our ecosystems and our food supply.

One-Sentence Summary: Robotic interaction with a honeybee colony influenced self-organized collective behaviors, enabling formation of a biohybrid society.

Main Text:

INTRODUCTION

Honeybees, like wasps, ants, and other social insects, establish large self-organizing colonies, often interpreted as being self-regulating "superorganisms" (*1*–*4*). These superorganisms are important stabilizers of ecosystems and are thus considered to be "keystone species" (*5*, *6*). For example, honeybee colonies' ecological effect through pollination service by foraging is substantial for terrestrial ecosystems (*7*, *8*). Honeybees are the most important eusocial pollinators (*9*), and hence crucial for our food supply (*10*,

11). In these ways, honeybees and their influence on ecosystems are a vital component for achieving the UN Sustainable Development Goals (SDG) (*8*, *12*), especially to SDG 2 (zero hunger) and SDG 15 (life on land). However, multiple anthropogenic stressors currently endanger honeybee populations (13, 14). Winter is the most critical season, when a high fraction of colonies die (*15–17*). During this period, a colony's objective shifts from growth and reproduction to form a thermoregulated cluster to survive (*18*). Although collective thermoregulation of honeybees during the summer is relatively well understood, less is known about how they respond to dynamic conditions during winter (*19*, *20*).

Interactive robotics is an approach to studying animal behavior (*21–24*), whereby robotic systems generate artificial stimuli enabling investigation of how individual or groups of animals respond. This brings potential advantages of automating experimentation (*25*), presentation of complex sequences of stimuli (*26*, *27*), and stimuli that are adapted according to animals' responses in a closed loop (*28*, *29*), potentially yielding a biohybrid society (*30*). But the approach is not without challenges. Developing such a system starts with identifying a suitable interaction pathway (*31*) such that the artificial agent is accepted by living animals. Therefore, important design goals include the need for minimal disruption to the natural behaviors (when not intentionally exerting influence), robustness to the animals and their local environments, and reliability for timescales spanning the behaviors of interest. Moreover, understanding the dynamics of specific behaviors may require multiple interactions (*26*, *27*), or interacting with multiple individuals (*30*, *32*). The latter point is especially pertinent in the study of collective behaviors expressed by honeybees in winter, which involves coordination of behaviors of thousands of animals (*33*) over periods of several months (*18*). Overcoming these challenges in developing robotics to modulate self-regulatory collective behaviors within a host bee colony could ultimately form a biohybrid superorganism. The robotic component of such a hybrid superorganism would enable us to better understand, and to interact with honeybee collective dynamics from within their society, even in challenging situations, such as during the winter period.

Here we present such a robotic device that thermally interacts with an entire colony of honeybees (*Apis mellifera carnica* Pollmann) comprising thousands of worker bees and a healthy queen (Fig. 1, Movie 1). We conducted experiments with this robotic system by observing and interacting with three colonies for several months during the 2020 and 2021 winter seasons. In a perturbation experiment, we demonstrated that the robotic device systematically controlled the location of the winter cluster. Moreover, through the sensor array we detected the thermal collapse of a weakened colony, that fell into a chill-coma state (*34*), and using thermal actuators, we were able to "resuscitate" the colony out of this unviable state, consequently extending its life. In another perturbation experiment, the robotic system autonomously measured colony reorganizations and reacted by generating new thermal stimuli to repeatedly reposition the cluster, thereby demonstrating a closed-loop animal-robot interaction. We validated, in an observation hive (see Fig. S5C), that identification of colony parameters and modulation of winter cluster organization were feasible with our embedded bio-compatible robotic system. Our system creates a pathway for field applications with conventional beehives, within which measuring colony parameters and applying appropriate actuation are challenging. Such application may

expand our knowledge of thermally mediated collective behaviors and emergent patterns in these pollinators vital to our ecosystems, to our agriculture, and consequently to our food security.

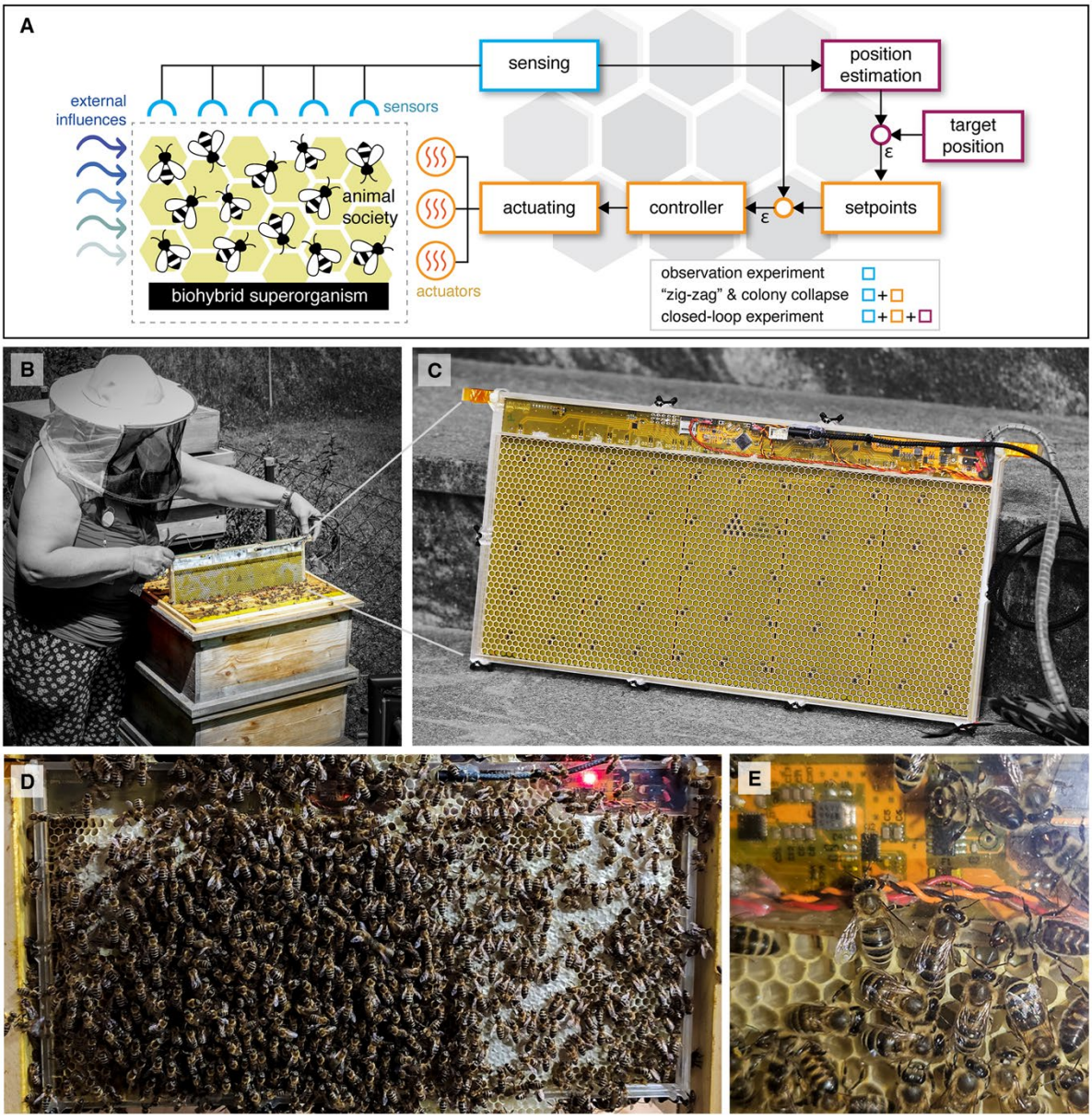

Fig. 1. A robotic system designed to conform to scientific and agricultural beehives. (**A**) Honeybee/robotic biohybrid superorganism overview including the regimes used in the experiments to control environmental (thermal) and behavioral (colony position) variables. (**B**) A photograph of a beekeeper performing a field verification of the robotic device fitting it into a standard box hive used in agricultural beekeeping. (**C**) A photograph of the assembled robotic system ready to be installed into a hive. In B and C, the beekeeper and the background were made black and white to emphasize the robotic device. (**D**) The robotic system operating in an observation hive. (**E**) A close-up image showing complete wax cells, and bees close to the electronics bay which is enclosed within transparent acrylic.

One environmental factor that highly influences honeybees is temperature. Accordingly, they exhibit diverse thermoregulatory strategies, building on individual (*35*, *36*) and social (*37–39*) mechanisms. For example, they tightly regulate the thermal microclimates to raise their young (*40*), and reduce high temperatures throughout their hives (*41*, *42*) and at localized hotspots (*43*). Moreover, honeybees respond to low temperatures by endothermic heat generation (*44*), especially within the winter clustering behavior (*45*), when a colony forms a dynamic self-regulating aggregate of thousands of bees that behaves like one single larger organism affording survival in cold climates. Recognizing the bees' sensitivity to temperature, prior research developed robotics that interacted with small groups of young honeybees, successfully modulating their behaviors with localized thermal stimuli under laboratory conditions (*46–48*). Therefore, a thermal pathway offers a promising candidate for a robotic platform to interact with entire colonies.

Our goal is to leverage robotic capabilities in scientific studies of honeybee collective dynamics, specifically, by means of robotic interactions that can provoke the animals' responses through modulation of localized thermal fields inside the hive. Understanding the emergent collective behaviors of colonies exposed to cold periods is difficult. This paper presents a robotic system that interacts with an overwintering superorganism that can be embedded into scientific and conventional hives. The robotic system demonstrated the ability to observe and quantify the thermal profiles of winter clusters during healthy and collapsing states. We also demonstrated the capacity to regulate colony level activity by influencing the movement of the bee aggregation in multiple colonies. The robotic system presented here has the capability to integrate into a honeybee colony and the potential to investigate their diverse collective thermoregulatory behaviors.

RESULTS

To evaluate the robotic system's ability to form a biohybrid society with a honeybee colony, we installed the system inside an observation hive populated with a queenright colony with approximately 4,000 bees (Colony A). Hives were situated in the Honeybee Field Laboratory in Graz (HFLG), Austria (see Methods). Firstly, we used the system to observe the natural activity of the colony (without the injection of any modulatory stimulus) to verify the capacity of the collected data to reveal specific collective behavior patterns. Secondly, we performed an experiment to assess whether the thermal actuators were able to emit meaningful stimuli to interact with the colony, to modulate its position in the hive. Thirdly, we identified the thermal collapse of a colony using the sensory system, and reported our efforts to revive the colony using thermal actuators. Finally, we tested the robotic system in an autonomous mode where it estimated and modulated the position of the colony.

Observing collective behaviors with a robotic system

To verify the system's capacity to monitor honeybee's thermoregulatory collective behavior, the system was utilized to observe a colony for one week in the 2020/2021 winter season, when all members of the colony tend to form a cohesive winter cluster. These observations (pictures and thermal data) are shown in Movie S1. When temperatures around the hive dropped below $T_{amb} = 11.2°C$, we observed the characteristic ellipsoidal shape of the winter cluster (*49*), with bees oriented inwards and aligned with

the temperature gradient (Fig. 2A) (*50*). The characteristic spatial organization of the winter cluster (*44*, *51*) is reflected in the thermal data collected by our system (Fig. 2B, Movie S1).

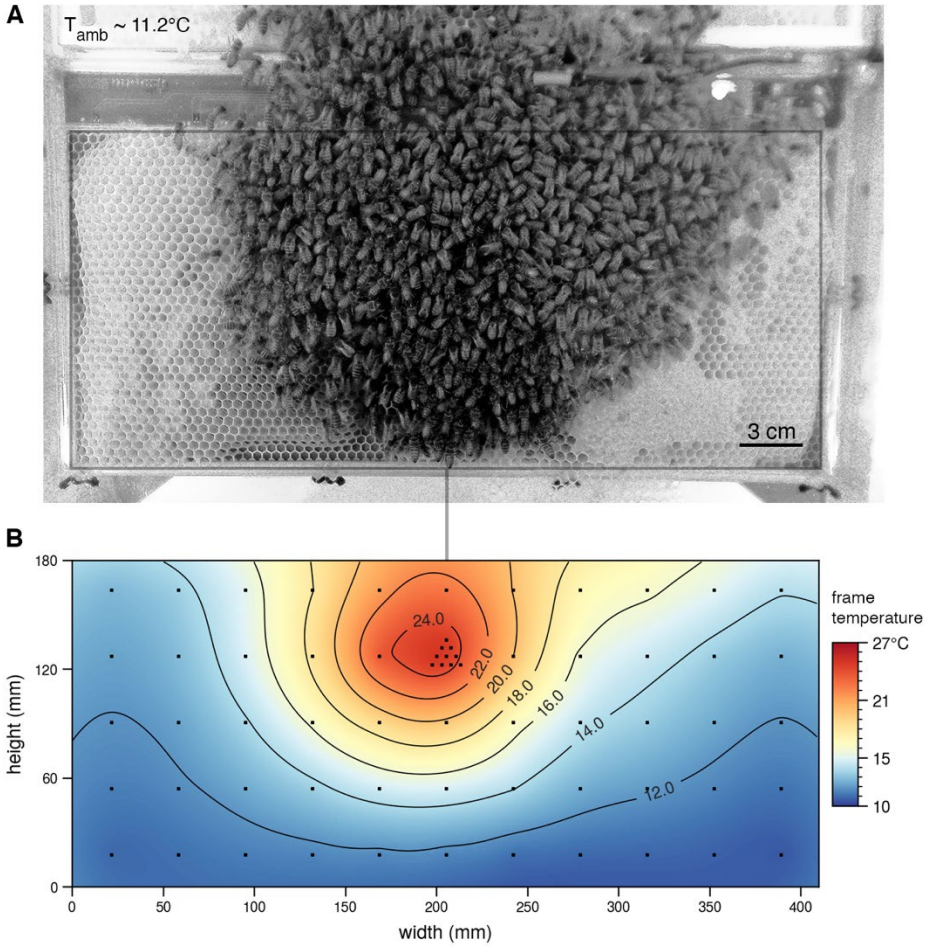

Fig. 2. A robotic system capable of observing collective thermoregulatory behaviors. (**A**) A photograph of a broodless bee colony displaying a winter cluster formation. (**B**) The associated thermal field generated by the linear interpolation of the data from 64 temperature sensors array (black markers).

Temporal dynamics of a winter colony

Honeybee thermal behaviors have differing temporal characteristics. Some have short durations (for example, individual bees heating brood cells (*40*)), whereas others can span over a period of months (such as winter clustering (*49*) and collective brood nest thermoregulation (*52*)). Hence, for a robotic system to integrate with a hosting colony, it must be able to properly sample the temporal evolution of the behaviors of interest.

To test whether the robotic system was able to capture the temporal dynamics of the winter cluster, we calculated the cluster's location and corresponding temperature values. We used computer vision to calculate the cluster's location using images and calculated the temperatures defining the cluster's outer edge T_{mantle}, the core contour T_{core}, and the core centroid T_{cen}, in 10 min intervals (n=1008). The temperatures on the perimeter of the winter cluster T_{mantle} (Fig. 3A, yellow) followed the ambient temperature patterns T_{amb}

(Fig. 3A, blue. Spearman correlation $\rho_s = 0.82$, lag 0.34h, $p < 0.001$) with a median offset of +3.8°C, suggesting that the colony adjusted its structure to remain inside a safe thermal range (*49*, *53*). When bees' body temperatures drop below T_{chill} =10°C (Fig. 3A, black dotted line), they fall into a comatose state, or "chill-coma", where they can no longer move or self-heat (*34*, *36*). Furthermore, the similarity in the slope values of the first-order regressions between T_{mantle} and T_{amb} against T_{ext}, rendering parallel curves (Fig. 3B, yellow and blue), reinforces the observation that the cluster adjusted to ambient temperatures (*53*, *54*). The mantle is where most ectothermic bees are located (*51*), and the cluster core hosts the majority of the endothermic bees (*44*). The border region between the core and the mantle displayed fast-changing dynamics (Fig. 3A, orange) but little sensitivity (that is, decoupling) to changes in ambient temperature (low slope in Fig. 3B, orange). The core centroid temperature T_{cen} (Fig. 3A, red), at the positions calculated from processed images, closely follows the maximum temperature of the thermal field (Fig. 3A, purple, $\rho_s = 0.98$, lag 0.17h, $p < 0.001$). Interestingly, T_{cen} is more sensitive to external variations than T_{mantle} (Fig 3B) observe the regression line slopes for T_{cen} and T_{mantle} in Fig. 3B).

Ambient temperature has a large influence on how a colony behaves, therefore making it an essential variable to be recorded. During the observation period, the external temperature T_{ext} ranged between –7.1°C and 7.1°C (Fig. 3A, dark blue) and remained below bee chill-coma threshold T_{chill} =10°C (Fig. 3A, black dotted line). The ambient temperature inside the field lab T_{amb} ranged from 8.0°C to 17.1°C (Fig. 3A, blue) and followed the changes in external temperature (Fig. 3B, dark gray, $\rho_s = 0.96$, lag 2.0h, $p < 0.001$) but with a positive median offset of 11.2°C. Inside the hive, the minimum temperatures measured in the populated frame T_{min} (Fig. 3A, gray) were very close to the temperature surrounding the hive T_{amb} (median offset 1.0°C). Note that there were brief periods where T_{min} was lower than T_{amb}, because T_{ext} is always below T_{amb} and cold air can flow into the hive through its entrance.

Spatial organization of a winter cluster

Winter clusters consist of thousands of bees (*55*, *56*), usually positioning themselves in thermally optimal locations, typically in the center of the hive (*49*, *54*). However, a cluster may also actively relocate itself towards honey reserves (*49*), needed for heating. Accordingly, a small number of sensing devices at fixed locations will fail to track the moving cluster throughout a season (*57*), but a dense array of sensors enables an accurate spatial representation of the signals generated by behaviors of interest.

We calculated the median thermal field of the cluster over the observation period (Fig. 3C). This thermo-spatial distribution captures the thermal gradient characteristic of winter clusters, with higher temperatures in the core than the periphery (*44*, *49*). By overlapping the image-based contours with the measured median thermal field, we found the representative median temperatures for the outer edge of the cluster $\overline{T}_{mantle} = 15.09 \pm 1.21$°C, the core perimeter $\overline{T}_{core} = 21.59 \pm 1.54$°C, and the core centroid $\overline{T}_{cen} = 27.39 \pm 3.03$°C (Fig. 3C).

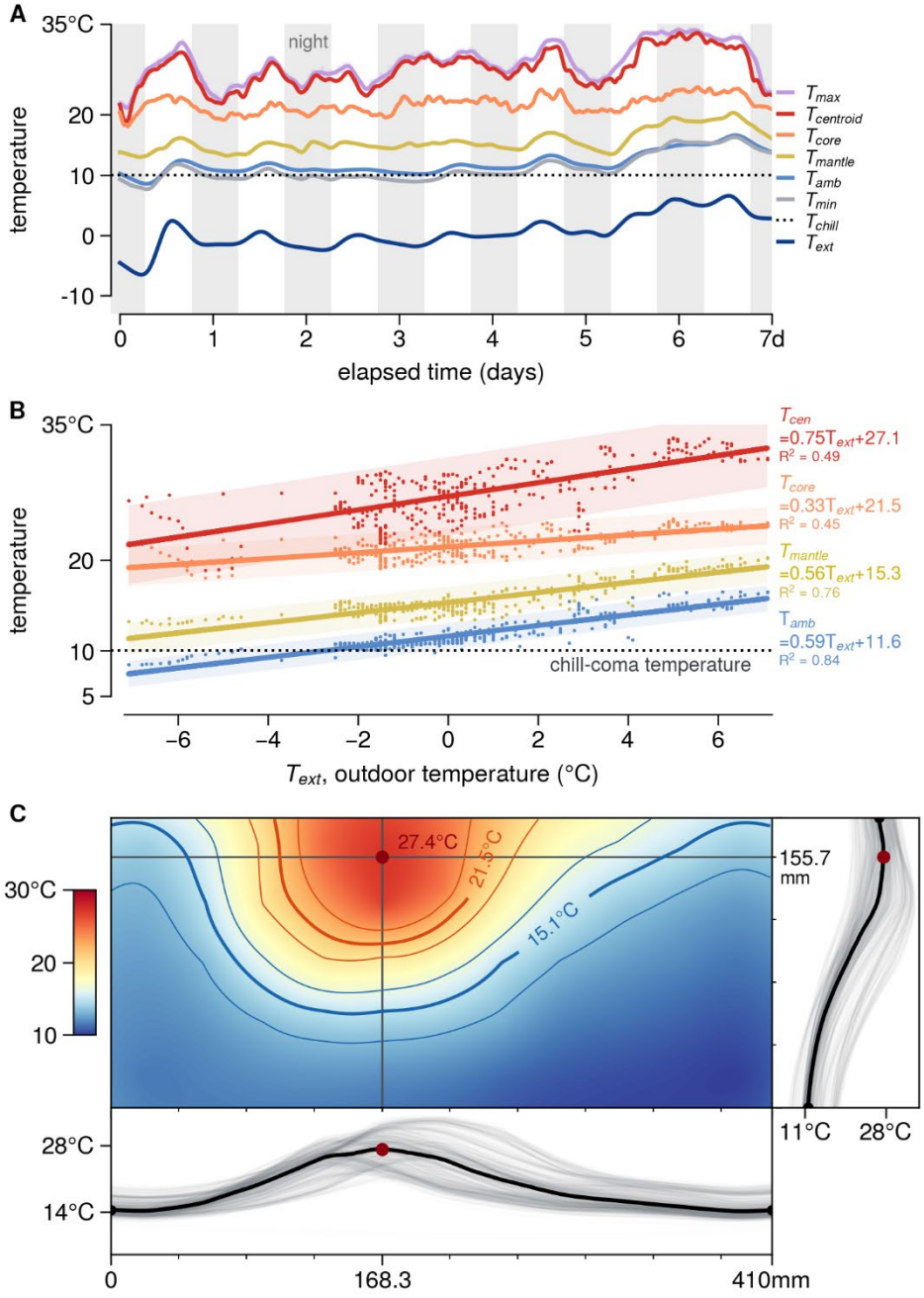

Fig. 3. Observation of the temporal and spatial dynamics of a winter cluster. (**A**) Temporal variation of different temperatures in the system. T_{cen}, T_{core}, T_{mantle} were calculated at 10-min intervals (n=1008), and T_{amb} and T_{ext}, were sampled every 30 min (n=335). Data smoothed with a trend filter. (**B**) Linear least squares regressions revealing the relationship between outdoor temperature and the temperature of the HFLG, T_{amb} (blue), cluster mantle contour, T_{mantle} (yellow), core contour, T_{core} (orange), and core centroid, T_{cen} (red). Color bands represent measurements' CI–95%. (**C**) Heatmap visualizing the median thermal field of the winter cluster during the observation period. Isotherms defining the outer edge of the cluster (blue) and the region of higher endothermic activity (orange) are shown. The median core centroid position is represented by a red circle. The thin lines delimit the isotherms uncertainty and are the median absolute deviations (MAD). Bottom and right panels depict the median thermal profiles of the horizontal and vertical transects crossing the core centroid (n=1008).

Robotic modulation of the winter cluster's position

For a robotic system to successfully integrate into an animal society, it requires not only the capacity to measure the state of the colony but also to emit relevant cues or signals to modulate behaviors of interest (*21–23*, *31*). The objective of the present experiment was to assess and characterize whether the thermal pathway could influence the animal collective. Specifically, we aimed to answer the question of whether the thermal cues emitted by the robotic system can affect the colony's collective position. We tested this with a perturbation experiment on colony A. We sequentially activated one of the five pairs of thermal actuators of the robotic system from one extremity of the frame to the other, creating a thermal stimulus with a zig-zag pattern (Fig. 4 and Movie S2). To attract the bees towards the actuator area, the controllers' objectives were adjusted to 25°C. This setpoint was warmer than the hive's ambient temperature (the experiment started with T_{amb} = 14.1°C), serving as a cue to attract bees to the warmer zone of the actuators, but lower than usual spring/summer temperatures. This avoids inducing potentially harmful behaviors during cold periods, such as onsets of foraging or breeding. Each actuator pair was active for a fixed period of 3 days. After each stimulation period, the actuators were turned off and the adjacent pair was enabled. This experiment lasted 51 days, with a 3-day initialization phase and 16 transitions.

To evaluate the movement of the cluster towards the thermal actuators, we computed the cluster's outer perimeter, its centroid position, and the horizontal distance of the centroid to the center of the actuator pairs (Fig. S1). When the actuator pair advanced to the next location (Fig. 5A, light yellow squares), the bee cluster followed it, which can be observed by how closely the centroid of the cluster follows the heated patches (Fig. 5A, red, blue, and Movie S2, Spearman correlation $\rho_s = 0.96$, lag 1.1 days, $p < 0.001$). This result also shows how similar the locations of the front and back sub-cluster are, with one mirroring the other ($\rho_s = 0.99$, lag 0, $p < 0.001$).

To increase the likelihood of system acceptance by the colony, the thermal actuators' controllers were designed to allow animals to participate in the control-loop (*24*). The temperature of endothermic bees is measured by sensors used in the control logic. This means that the balance of heat produced by the bees versus by the robotic agent is affected by the bees' behaviors. Consequently, instead of a constant power injection, the amount of delivered energy was influenced by T_{amb} and the animals (Fig. 5B, yellow). During the experiment, the active thermal actuators operated at 51% of their maximum capacity (median power 0.77 ± 0.27 W, n=34 activations, power limited to 1.5 W). All the thermal actuators dissipated a total energy of 6.13 ± 0.59 MJ (median ± MAD) in 51 days. We estimate this energy to correspond to approximately 68 g/day of honey, equivalent to 15% of the energetic demands of the colony (see Supplementary Methods for details of the derivation).

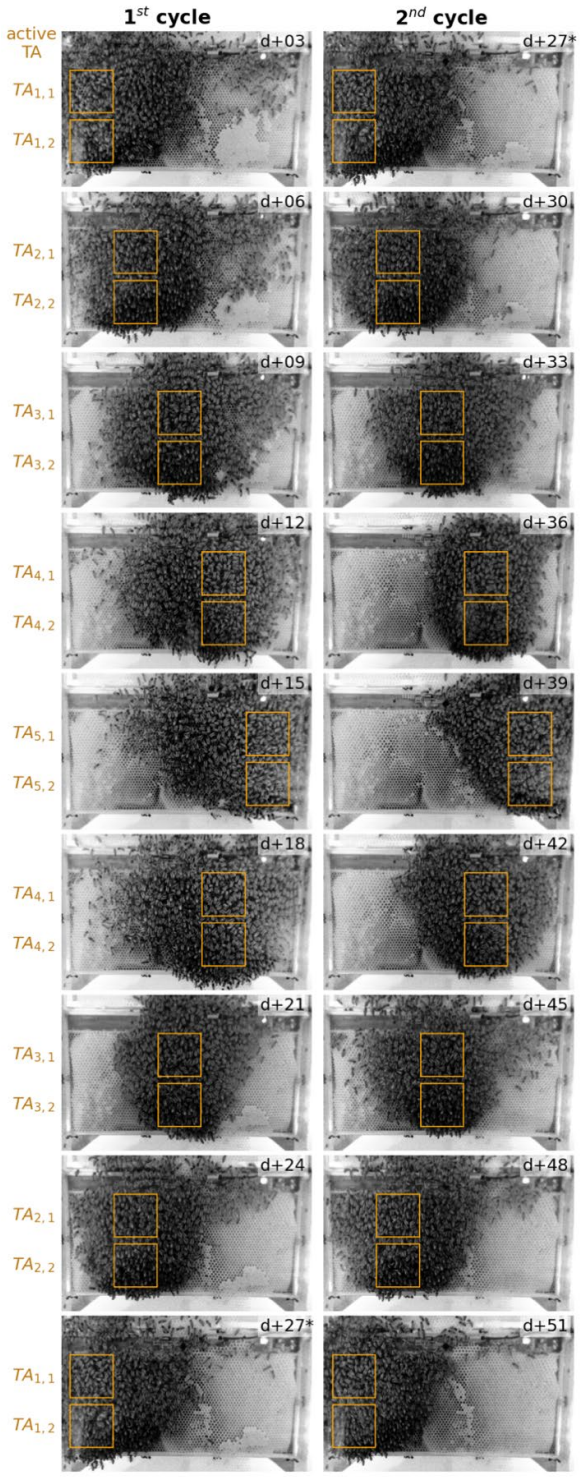

Fig. 4. Thermal stimulation to modulate the winter cluster's position. Timelapse showing the 51 days of experimentation, depicting an aggregation of bees following the thermal stimuli emitted by pairs of actuators organized in five columns (orange). Thermal actuators indexed following the convention: $TA_{column,\ row}$. Each frame above corresponds to the end of an activation period, every 3 days, with initial day d_0 = 08-Dec-2020. The last image of the first cycle (d+27, left-bottom) is duplicated as the starting image of the second cycle (right-top). Only the front side of the cluster is shown, since the back sub-cluster followed a similar trajectory.

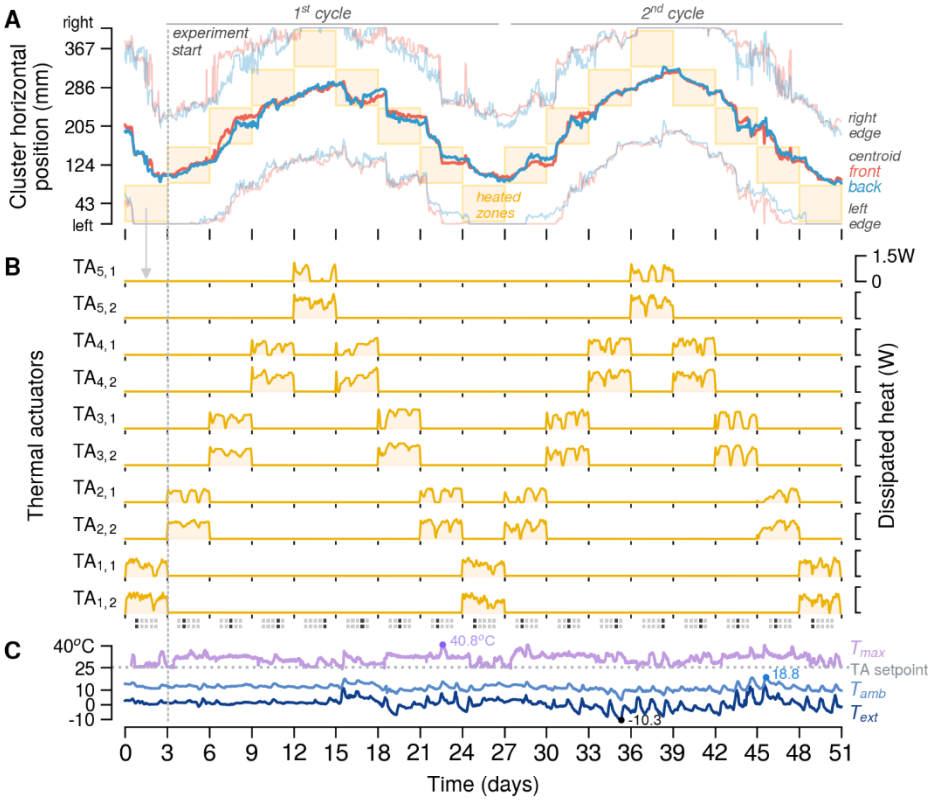

Fig. 5. The influence of the robotic system on honeybee collective position. (**A**) The change in position of the cluster with respect to thermal actuators. The horizontal centroid position and the cluster's left and right extreme positions of the back (blue) and front (red) sub-clusters are shown. Cluster perimeter and centroid were calculated every 30 min. (**B**) Thermal actuator activation sequence and injected power over the course of the experiment (yellow). Actuator data sampled every 10s and trend filtered. (**C**) External T_{ext} (dark blue), HFLG T_{amb} (blue) and T_{max} (purple) temperatures, sampled every 30 min.

The broad temperature range observed inside the HFLG, T_{amb} from 3.1°C to 18.8°C (Fig. 5C), did not impair the robotic device's capacity to modulate the colony position observed by the cohesiveness of the bees cluster (and the weak negative monotonic correlation between T_{amb} and the cluster centroid, with a peak correlation of $\rho_s = -0.26$, $p < 0.001$, over a 10-day window). When the ambient temperature increased (such as on day 45), the winter cluster expanded and was less influenced by the actuators' thermal cues, which can be seen by the higher variability in the cluster's horizontal position (Fig. 5A).

The cluster moved neither immediately nor constantly towards the new stimulus (Fig. S1). Rather, it took 11.6 ± 1.5 hours to start moving (considered after the cluster center moved 5 mm from the previous position), and 15.1 ± 10.8 additional hours to enter the zone of the newly activated actuator (Fig. S1A). The cluster speed increased during the night to a maximum of 9.3 cm/day (Fig. S1B). The cluster could align itself with active actuators in the center of the frame but to a lesser degree at the edge of the hive (Movie S2; Figs. 5A and S1C).

Winter colony collapse and robot-mediated resuscitation

Stressed or weakened colonies are more susceptible to colony collapse (*58*). No other period is more critical than the winter when a high percentage of colonies die (*15–17*). When temperatures drop inside the colony, bees can fall into a chill-coma which could lead to their deaths (*59*). In this state, bees can no longer self-heat, but the state is reversible if they are warmed by an external source (*34*). Inducing such a state would be unethical, but since it occurred to a colony under observation by our robotic system, we were able to test the robot-mediated augmentation of this animal society. Exploiting the sensing and modulating capabilities of the robotic device demonstrated above, we intervened in a colony identified at a critical state. During the winter of 2021/2022, a standard treatment against varroosis (*60*) was performed in an effort to strengthen Colony B (spraying 3 ml of 3.5% oxalic acid). Soon after the application of oxalic acid (time t_0), the robotic device observed changes in the endothermic area ($\overline{T}_{core} > 21.5$°C, see above). Approximately 6 hours later, the area started to shrink until it disappeared at t_0 +11.3h (Fig. 6B), indicating that bees had stopped their endothermic activity, and eventually fell into chill-coma. The decrease in endothermic activity is also evident in the maximum temperature T_{max} (Fig. 6C, orange), which displayed a declining trend a few hours after the treatment. Moreover, the recorded images revealed no visual signs of motor activity, with bees standing still (Movie S3).

Approximately 5 hours after the robotic system indicated temperatures below the chill-coma threshold, T_{chill} =10°C, we decided to try resuscitating the bees using the thermal actuators (Fig. 6C, faded curves). We manually applied a multi-step heating procedure that re-animated the comatose bees, which allowed them to re-aggregate, and then guided them using robotic modulation towards honey supplies on the opposite side of the hive. About 2 hours after activating the thermal actuators, we observed bees regaining motion, and 20 hours later the surviving bees regrouped into a new cluster. Despite the colony not ultimately surviving (likely due to the loss of the queen), our "resuscitation effort" avoided its immediate collapse and extended its life for over 2 months (Movie S3).

The robotic system showed that the winter cluster is not a static aggregation. During the 30 days prior to the oxalic acid treatment, the cluster's point of maximum temperature moved considerably, d_{Tmax} = 21.3 cm (Fig. 6E). This implies that any single sensor placed inside a hive would have failed to capture the thermal signature of the cluster (Fig. 6D gray curve). But, since our robotic devices possess arrays of temperature sensors, they can accurately reveal the cluster's repositioning.

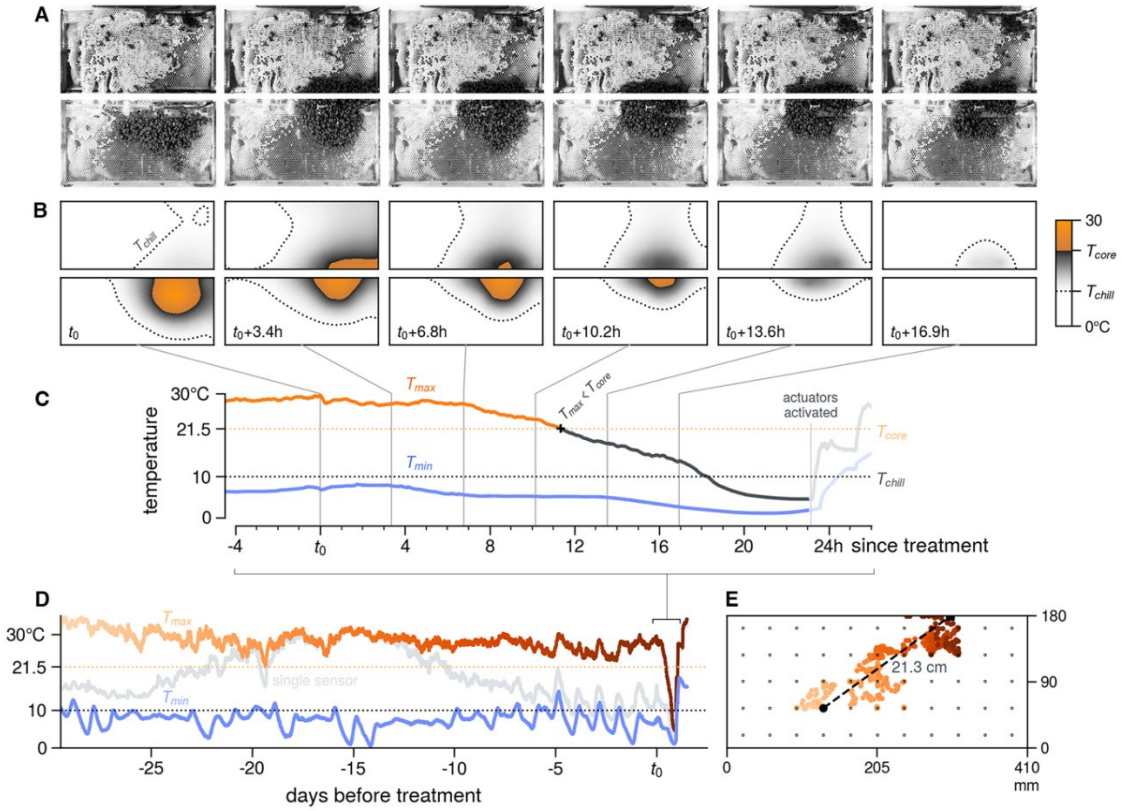

Fig. 6. The collapse of a honeybee winter colony can be detected by its thermal dynamics. (**A**) Images showing the colony during thermal collapse. When the cluster falls into a chill-coma it can maintain approximately the same shape of a healthy thermogenic cluster. Therefore, diagnosing a colony in a critical state by visual inspection, especially with still images, can be difficult. (**B**) Temporal evolution of the endothermic area (orange region). The black dotted line defines the isotherm at chill-coma threshold, T_{chill} =10°C. (**C**) Time series of the minimum temperature T_{min} (blue) and maximum temperature of the frame T_{max}, which is colored orange whenever $T_{max} > \overline{T}_{core}$, implying the presence of a thermogenic core in the winter cluster. T_{max} color changed to gray when $T_{max} \leq \overline{T}_{core}$. Around t_0 + 23h all thermal actuators were manually activated causing the T_{max} and T_{min} to rise. (**D**) Evolution of the cluster's maximum temperature T_{max} over a 30-day period prior to t_0 (orange). The gray curve represents the temperature of a single sensor, in the center of the frame, illustrating the necessity of multiple sensors. The blue curve shows T_{min}. (**E**) Spatiotemporal evolution of the point of maximum temperature in the cluster, d_{Tmax}, over the period of 30 days (time is encoded with the same colors as panel D).

Autonomous closed-loop interaction

The synthesis of a biohybrid society relies on the capacity of living and artificial agents to interact. With an aim of testing whether the robot could use its sensory information to perceive colony states and autonomously generate new stimuli in response, we devised a perturbation experiment to attract the winter cluster to one of two designated regions, defined as zone L (left side) and zone R (right side), and comprised of four thermal actuators each (Movie S4). Once the system detected that the cluster's residency time within one of the target zones was longer than 12 hours, it activated the thermal actuators of the second zone with the intention to attract bees there. The robot relied solely on its thermal sensing array to estimate the cluster's position.

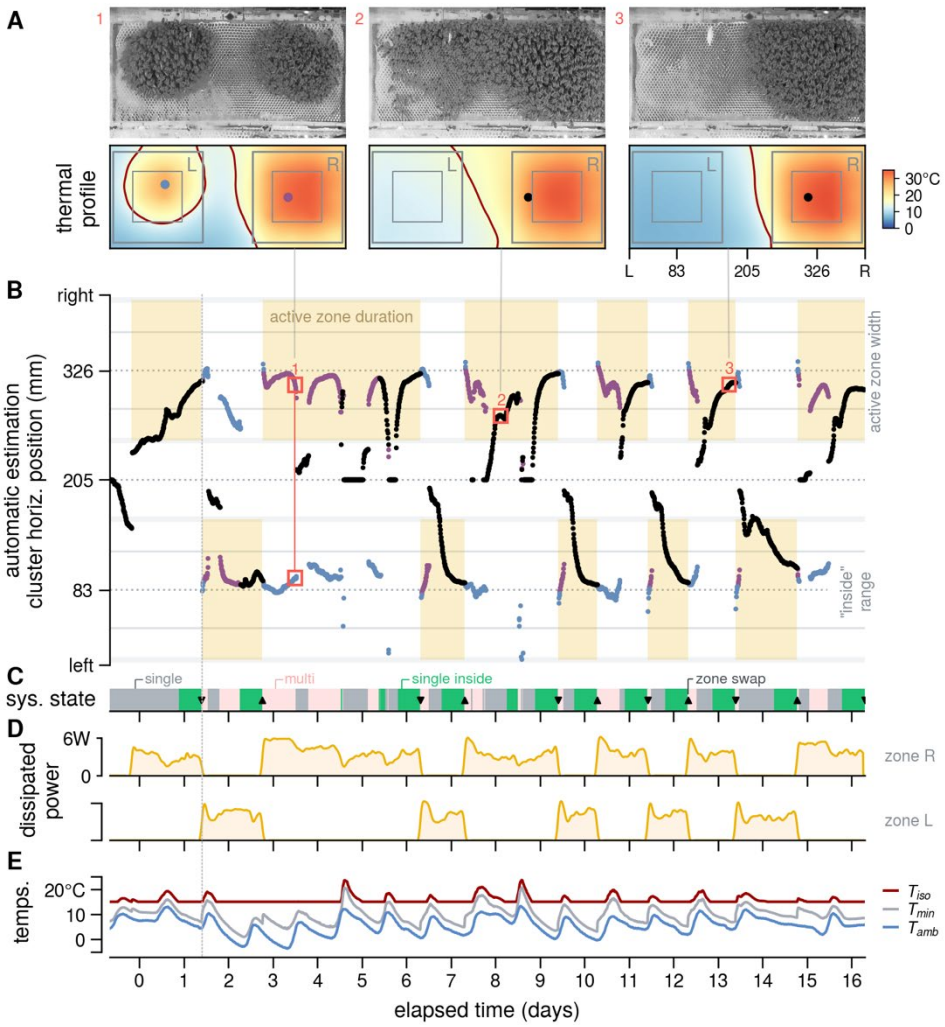

Fig. 7. Autonomous interaction between robotic agent and animal colony. (**A**) Examples of three frequent states detected by the system: (1) when the cluster was split in two or it was far from the active zone, two thermal hotspots are observed (the bee cluster and the actuators). This condition does not allow the robotic system to distinguish the true location of the winter cluster; (2) when just one maximum is defined but its centroid is outside the active zone; (3) when the detected contour is inside the active zone. (**B**) Time series of the estimated position of the cluster in response to the activated thermal zone (orange patches). Single centroids are depicted by black markers (•). When two centroids were estimated, their positions could be represented by purple and blue markers (••). (**C**) Autonomously identified states: cluster outside (gray) or inside (green) new stimulated zone; or undefined colony position where multiple centroids were found (red). (**D**) Total dissipated power by the four thermal actuators of each zone (orange curves). (**E**) Relevant temperatures for the biohybrid interaction: T_{iso} (red) is computed from T_{min} (gray) that serves as a proxy for T_{amb} (blue).

During a period of 16 days, Colony C repeatedly responded to stimuli generated by the robotic device (Fig. 7B). Each time the system was able to find the cluster's centroid position and detect that bees were inside the selected zone (Fig. 7C, green segments) it generated a new thermal landscape. In contrast to the fixed-time regime used in the modulation experiment (Fig. 4), here the robotic system and animals jointly defined the transitions in thermal stimuli. Specifically, the robotic system waited for the animals to adjust to the stimulus which had a variable timespan as expected within natural societies.

The median active zone residency time was 29.8 ± 9.4 hours (range 21–85 h, *n*=10), with a residency time at zone R, 36.4 ± 16.2 h (*n*=5), slightly longer than zone L, 23.6 ± 3.9 h (*n*=5). Altogether these results demonstrate that our robotic device is able to systematically modulate colony position autonomously, based on successful perception of the animals and effective stimulus generation.

DISCUSSION

Our results imply that robotic systems are capable of integrating and interacting with full-sized honeybee colonies. The presented robotic device can observe the thermal characteristics of the winter cluster (Movie S1), consistent with prior observations (*44*, *49*, *54*), with high temporal and spatial resolution. Moreover, it is able to measure the thermal profile of a collapsing colony, providing potentially valuable data for future predictive systems of colony health. Our study yields two key results. Firstly, the robotic platform's ability to systematically reposition the cluster, formed by thousands of bees, following a predefined pattern over 51 days (Fig. 1 and Movie S2). Secondly, using the robotic system in an autonomous mode, we successfully demonstrated that it was capable of perceiving the animals' position and consistently influencing their movement for 10 transitions over 16 days (Movie S4). Key properties of the presented system are its biocompatibility, dense array of sensors, and thermal actuation in close proximity to the cluster. These characteristics enable the robotic system to successfully interact with intact honeybee colonies over substantial periods, including the control of the movement of a large number of animals.

The proximate mechanisms of winter cluster thermoregulation including displacement of the bees are still unresolved research questions. Stabentheiner et al. (*44*) identified competing hypotheses that differ concerning the mechanisms essential to explain the cluster organization. Studies using in silico models addressing the within-cluster self-regulation (*61–65*) and formation (*63*) have been based and validated on data from experiments with entire honeybee clusters subjected to various uniform ambient temperatures (*44*, *49*, *66*). Our system can generate nonuniform thermal stimuli that can be located inside or outside of the cluster and can move over time. These stimuli offer possibilities for experimentation to better understand behavioral mechanisms and thus stimulate refined modeling. For instance, our results showed several observations inconsistent with some assumptions made in state of the art models, such as individual positive thermotaxis of bees (temperature gradient-climbing) (*61–65*). Specifically, the cluster was able to sense a localized thermal cue that was outside of its own perimeter. For the cluster to relocate to such newly-appearing cues, the new area was only reachable by traversing a local temperature minimum in several cases (such as in Fig. 7A). These observations reject a hypothesis of individual thermotaxis towards a preferendum. New models may incorporate a method of representing bees moving outside of the cluster, such as through an additional state that relaxes the need for thermotaxis to allow random exploration. A model including this feature may be able to reflect the local minimum traversal dynamics observed – although care would be needed to avoid undermining the existing ability to maintain a cluster.

Although our system was developed to investigate collective behaviors, we can nonetheless envisage some immediate applications in supporting the colony. For example, the robot's sensing and actuating capabilities allowed us to manually execute a "resuscitation maneuver" on a colony under observation. This action prevented the immediate death of the colony, and allowed the remaining bees to regain mobility and to reaggregate into a single compact cluster. Since the rescuing heating was not switched on until about six hours after the bees fell into a chill-coma (when $T_{max} < T_{chill}$), a large number of bees and the queen were lost, removing the colony's chance of repopulating. Ultimately, the number of surviving bees was already too low to sustain the colony until the foraging season commenced in the next spring. Despite the colony's ultimate demise, the robotic device managed to keep the bees alive for over two months. This gives hope that future autonomous colony-health monitors will enable the application of supportive heating at early stages of the collapse increasing the probability of a full recovery. Further investigation is required to understand the effects of prolonged heat injection on aspects including the ratio of endothermic (active) to ectothermic (passive) bees, as well as the colony metabolic consumption (*67*). Such an understanding should inform the development of efficient strategies for robotic intervention. More generally, the observational and modulatory capacity of such robotic systems, tightly integrated into a hosting honeybee colony, could be beneficial in several ways. Observations of the animal society can contribute to design data-based health monitoring systems (*68*, *69*). Modulation systems could be utilized in automating heat treatments against varroa (*70*), or to actively intervene in a distressed colony to try to revert its collapse. For instance, during winter, colonies can die from starvation despite honey stores remaining in unreachable cold regions (*51*), and an array of embedded thermal actuators could provide safe passages to make them accessible. Despite the single instance of the presented robotic intervention, temporarily reverting the fate of a collapsing colony, this result emphasizes how robotically-enhanced organisms could be more resilient to challenging habitats.

Observation hives provide an invaluable way to study behaviors from intact colonies, which interact with their natural ecosystems, in otherwise obscured regions of a hive (*39*, *71*). However, they bring some drawbacks, including an increased risk of luminous contamination inside the hive , and the reduced thermal isolation when compared to tree trunks or box hives (*18*, *72*). Furthermore, these hives limit populations to 4,000–20,000 individuals (*18*). Moreover, in observation hives, frames are usually stacked vertically, instead of parallel to each other, constraining bees to form more disk-like clusters during cold periods. However, our system is compatible with box hives (Fig. 1B) where multiple robotic devices could be placed parallel to each other. We see an opportunity for experiments with colonies that adopt more diverse topologies including those seen in apiculture, as well as in summer seasons during which honeybees exhibit various other collective behaviors. Application in field scenarios could ultimately support an important keystone species on a large scale, since one colony can forage and pollinate more than 100 km^2 (bees fly up to 14 km) (*18*). This way, such autonomous robotic systems can also contribute to ecosystem stabilization and agricultural improvements.

MATERIALS AND METHODS

Robotic system design

The robotic system comprises three sub-modules: the system orchestration and data processing, the thermal sensing, and the thermal actuation. For orchestrating the execution of low-level controls and high-level communication with external users and devices, we used an ARM Cortex-M4 32-bit microcontroller (MCU, STMicrosystems STM32F405). In the MCU, a real-time operating system (RTOS, ChibiOS v19.1) provides a multi-thread scheduler to run applications in a single-core processor. To make available an external interface to data, code, and commands between the robotic device and users or devices outside the hive, a USB communication channel was made accessible (Fig. S5A).

Thermal sensing

We selected a small (2.0 mm × 2.0 mm × 0.8 mm) silicon-based temperature sensor (TI TMP117) that fits within inside a honeycomb cell (preliminary trials with larger sensors caused bees to avoid the area nearby). This sensor returns a 16-bit temperature value with a resolution of 7.8125×10^{-3} °C, and can operate in the range of –20°C to 50°C with an accuracy smaller than ±0.1°C (*115*). The robotic device was equipped with 55 temperature sensors arranged in a 5 × 11 array with vertical and horizontal spacings of 36.4 mm and 36.8 mm respectively (Fig. S5B). In addition, to allow the investigation of finer details of thermal fields, a nine-sensor high-density patch was positioned at the central axis of the frame (Fig. S5B), bringing the total number of sensors to 64. Since these sensors use an I_2C digital communication bus, with the possibility of four different identification addresses, a circuit with two 8-channels multiplexers (TI TCA9548A) was devised to connect all 64 sensors to a single I_2C port in the MCU (Fig. S5A).

Thermal actuation

Bees adjust the metabolic intensity of specific thermogenic activities to the hive microclimate and social conditions (such as winter clustering and brood caring). Generally, the average maximum metabolic rate is approximately 115 W/kg at 10°C and decreases at higher temperatures (*35*, *45*, *55*, *73*). To allow our system to generate thermal cues with intensities similar to natural behaviors, we distributed 10 thermal actuators (2 × 5 array), in the bee-occupied area of the robotic device, with a total dissipation capacity of 158 W using a 12 V supply, similar to the peak metabolic rate of a 1-kg honeybee colony (~7,700 bees (*74*)). Actuators were designed as meandered copper trace resistors R_{act} that warm up via Joule heating when current flows through them ($P_{heat} \propto I^2 R_{act}$). Each actuator consists of a 4,852 mm long copper trace, laid out over a square area with 74.7 mm sides, resulting in a 9.1 Ω resistance.

Each actuator is powered with 12 V from the system main power supply, and it is individually modulated by the microcontroller via pulse-width modulation. This control signal is sent to a gate driver chip (TI UCC27517A) that enables the fast actuation of a power MOSFET with low R_{ON} (Vishay SiSS12DN) and connected to each thermal actuator (Fig. S5A). We numerically implemented a proportional integral differential (PID) controller for each actuator's duty cycle, although note that the system can accommodate diverse control strategies.

Mechanical construction

To allow the instrumentation of hives used in science (observation hives) and agriculture (box hives), the robotic system was designed in the form of a Zander beekeeping frame (420 mm × 220 mm, Fig. S5B). The frame structure consists of a sandwich of six layers with a printed circuit board (PCB) made of 1.6 mm FR-4 (epoxy and fiberglass) in the center. The PCB is surrounded by six laser-cut layers, where the four outermost layers are made of plexiglass and the two closest to the center are made of 1 mm thick wood laminate. The wood layers exhibit a hexagonal pattern to serve as a honeycomb construction template for worker bees (Fig. 1), with cells presenting minor and major inner axes of 4.55 mm and 5.25 mm respectively. The monitored and actuatable area of the frame has a surface area of 410 mm × 180 mm and is fully covered by the hexagonal mesh. The in-hive atmosphere is very humid, and bees can be very protective against foreign bodies (for example, by chewing soft materials or covering parts with propolis). Therefore, to protect the temperature sensors installed inside cells, we coated them with a 50-75 μm acrylic resin layer (MG chemicals 419D) and electronics and connectors were placed inside the protected "electronics bay", in the upper 30 mm of the frame.

When designing the elements of the robotic system including control software, hardware, and materials, we were committed to ethical principles to preserve the animal's welfare and we considered the consequences of mixing robotic devices and living organisms (see Supplementary Discussion "Ethical considerations").

Robotic system preparation

To prepare the robotic device for experimental colonies' integration, the hexagonal mesh on both sides of the honeycomb was coated with melted beeswax. This structure led to better bio-acceptance and provided initial building material for the construction of honeycombs (Fig. 1). Once prepared, the devices were inserted either into a populated box hive, by replacing one of the nine conventional Zander combs (Colonies B and C), or directly into an observation hive with a bee colony (Colony A). Robotic systems that were added to established colonies in box hives had fully drawn cells constructed after 10 to 14 days and were then transferred to observation hives. Since there is comparatively less space in an observation colony, hence fewer bees, the construction of the combs took slightly longer there (~21 days). All experiments were made in observation hives in the Honeybee Field Laboratory Graz (HFLG), at the Botanical Gardens of the University of Graz, in Graz, Austria.

Animals, colonies & hives

Colonies of *Apis mellifera carnica* Pollmann, bred for commercial use by the Styrian Beekeeping Center, Austria, were established at the University of Graz for the purposes of scientific research. According to the principles of animal care of the University of Graz, the ethics commission of the university as well as the Austrian Animal Experiments Act (Tierversuchsgesetz 2012 - TVG 2012, 1. Abschnitt, §1), no ethical approval is required for experiments with insects. The animals received appropriate care from a professional animal keeper before, during and after the observations and experiments. A queen was introduced to the colony and acclimatized in a queen cage for three days before being

released to roam freely in the colony. During the entire experimental period, the bees were fed ad libitum with 73% sucrose solution.

Three colonies were used in this study. Colony A was used in the observation and modulation experiments, performed during the 2020–2021 winter season, and with an estimated initial size of approximately 4,000 bees. The system was installed in the hive on 01-August-2020 where preliminary tests and observational experiments were conducted, accounting for a total of 180 days inside the colony (preliminary and experimental phases). For this colony, the data presented above are from 01-December-2020 to 28-January-2021. Measurements from Colonies B and C were taken during the 2021–2022 winter season and presented in the colony collapse and closed-loop experiment results respectively. These colonies were estimated to have an initial size of 5,000 bees.

In the experiments, we used observation hives (w×h×d = 53 cm × 68 cm × 11 cm) containing two vertically stacked Zander frames. In colonies A and C, we used one robotic system, and in Colony B two were used. Pipes installed in the lower part of the hives gave bees access to the exterior. Both faces of the hives were covered by 4-mm anti-reflective glass windows (Conturan Magic), allowing the colony activity to be recorded (Fig. S5C).

Experimental setup

At the observation hives in the HFLG, each robotic device was controlled by a dedicated single-board computer (SBC, Raspberry Pi 4) located outside the hive. In addition, two extra SBCs controlled four cameras (Raspberry Pi High Quality Camera, with the 6-mm CS-mount lens with removed IR filter) facing the combs from the front and backside. Since bees are not sensitive to infrared (IR) light, hives were illuminated by 12 IR lamps (Synergy 21 LED retrofit 4×1W IR security) equipped with paper diffusers. The dedicated SBC orchestrated the behavior of the connected robotic device (via its MicroPython interface), collected, processed, stored measurements, logged system events, recorded images and finally uploaded the data to a desktop PC (located in the HFLG).

To allow the analysis of the influence of the ambient surrounding the colony during the experiments, we installed a weather station (Ecowitt Eurochron EFWS 2900) near the HFLG. The relevant variables to this research were the external temperature T_{ext} and the ambient temperature inside the HFLG T_{amb}, measured through a wireless dongle connected to the weather station. Both temperatures were recorded in intervals of 30 minutes.

Closed-loop experiment

Prior to the experiment, actuators $TA_{3,1}$ and $TA_{3,2}$ were activated for 3 days to move the colony to the center of the frame. Then, from 09-January-2022 to 26-January-2022, the robotic system installed within Colony C operated autonomously. The robotic device was programmed to attract bees to one of the two defined zones comprising four thermal actuators, with maximum combined heat dissipation of 6 W and regulated to 30°C when active. Once the system measured the cluster residency time inside the desired zone to be longer than 12 hours, it would deactivate its thermal actuators and activate the actuators of the opposite zone. The robotic system was programmed to estimate the position of the bees based on their thermal signature. This used an isotherm (T_{iso}) to delimit a contour that

would represent the cluster's position. Following preliminary work with a constant T_{iso} that failed to track the cluster when ambient temperatures (and consequently T_{min}) were warmer than T_{iso}, we designed a simple piecewise-linear function to define T_{iso}. Specifically, T_{iso} adapted to changes in ambient temperature. For T_{min} values below 11.2°C, $T_{iso} \leftarrow$ 15°C. For higher values of T_{min}, the isotherm threshold adapted as $T_{iso} \leftarrow 0.92 \cdot T_{min} + 4.7$, after the linear regression between T_{mantle} and T_{amb} (closely related to T_{min}).

Statistical methods

Sample sizes are described in each result section text and in figure legends. A nonparametric kernel density estimator was used to compute probability density distributions for the observation experiment (Fig. S2) and the perturbation experiments (Figs. S3, S4). If not indicated otherwise, measurement estimators are stated as the sample median and after the symbol ± the uncertainty is expressed by the robust estimator of spread MAD (median absolute deviation), and found by: $\mathrm{MAD}\{x_i\} = 1.4826 \cdot \mathrm{median}\{||x_i - \mathrm{median}\{x_i\}||\}$ (*118*). Confidence intervals at the level of 95% represent the uncertainty of the linear regressions presented in Fig. 3. In some noisy time series, we applied a trend filter (for example, Figs. 3A, 5B), and whenever the level of temporal similarity between series was stated, we computed it via a time lagged Spearman rank correlation (see Supplementary Methods "Trend filtering" and "Time series relationships").

Data analysis

Optical data was sampled at 4-second intervals from both sides of the hives. The collected images were undistorted and contrast-enhanced via a sequence of algorithms. To understand the cluster structuring, images were automatically segmented to identify areas containing bees (through an adaptative background subtraction method) and zones with bees presenting different levels of motility (via dense optical flow). Details of these methods are included in the Supplementary Methods "Visual data sampling and processing".

The thermal fields used in the analysis were generated from the linear interpolation of the 64 temperature values provided by the robotic systems' sensor array. For the extraction of the thermodynamics of different regions of the cluster, we sampled the thermal field at the core, mantle, and peripheral positions extracted from the optical analysis (see Supplementary Methods "Thermal data analysis").

Supplementary Materials

Supplementary Methods
Supplementary Discussion
Fig. S1. Dynamics of cluster motion towards thermal stimuli.
Fig. S2. Data distributions for the observation experiment.
Fig. S3. Data distributions for the collective position modulation experiment.
Fig. S4. Data distributions for the autonomous closed-loop experiment.
Fig S5. Structure and design of the robotic honeybee comb.
Movie S1. Time-lapse of the observation experiment showing pictures and thermal profiles of the winter cluster.

Movie S2. Time-lapse showing modulation of the winter cluster's position.
Movie S3. Annotated video depicting the evolution of a winter cluster, from the formation of a cluster until the "resuscitation" effort after the collapse of the colony.
Movie S4. Autonomous closed-loop collective position modulation experiment depicting visual, thermal and robot-processed data.
References: (*75–90*)

References and notes:

1. B. Hölldobler, E. O. Wilson, *The superorganism: the beauty, elegance, and strangeness of insect societies* (WW Norton & Company, 2009).

2. R. F. A. Moritz, S. Fuchs, Organization of honeybee colonies: characteristics and consequences of a superorganism concept. *Apidologie*. **29**, 7–21 (1998).

3. T. D. Seeley, The Honey Bee Colony as a Superorganism. *Am. Sci.* **77**, 546–553 (1989).

4. T. D. Seeley, P. K. Visscher, T. Schlegel, P. M. Hogan, N. R. Franks, J. A. R. Marshall, Stop Signals Provide Cross Inhibition in Collective Decision-Making by Honeybee Swarms. *Science*. **335**, 108–111 (2012).

5. A. Traveset, C. Tur, V. M. Eguíluz, Plant survival and keystone pollinator species in stochastic coextinction models: role of intrinsic dependence on animal-pollination. *Sci. Rep.* **7**, 6915 (2017).

6. M. S. Nash, J. P. Anderson, W. G. Whitford, Spatial and temporal variability in relative abundance and foraging behavior of subterranean termites in desertified and relatively intact Chihuahuan Desert ecosystems. *Appl. Soil Ecol.* **12**, 149–157 (1999).

7. L. Elizalde, M. Arbetman, X. Arnan, P. Eggleton, I. R. Leal, M. N. Lescano, A. Saez, V. Werenkraut, G. I. Pirk, The ecosystem services provided by social insects: traits, management tools and knowledge gaps. *Biol. Rev.* **95**, 1418–1441 (2020).

8. V. Patel, N. Pauli, E. Biggs, L. Barbour, B. Boruff, Why bees are critical for achieving sustainable development. *Ambio*. **50**, 49–59 (2021).

9. R. Rader, I. Bartomeus, L. A. Garibaldi, M. P. D. Garratt, B. G. Howlett, R. Winfree, S. A. Cunningham, M. M. Mayfield, A. D. Arthur, G. K. S. Andersson, R. Bommarco, C. Brittain, L. G. Carvalheiro, N. P. Chacoff, M. H. Entling, B. Foully, B. M. Freitas, B. Gemmill-Herren, J. Ghazoul, S. R. Griffin, C. L. Gross, L. Herbertsson, F. Herzog, J. Hipólito, S. Jaggar, F. Jauker, A.-M. Klein, D. Kleijn, S. Krishnan, C. Q. Lemos, S. A. M. Lindström, Y. Mandelik, V. M. Monteiro, W. Nelson, L. Nilsson, D. E. Pattemore, N. de O. Pereira, G. Pisanty, S. G. Potts, M. Reemer, M. Rundlöf, C. S. Sheffield, J. Scheper, C. Schüepp, H. G. Smith, D. A. Stanley, J. C. Stout, H. Szentgyörgyi, H. Taki, C. H. Vergara, B. F. Viana, M. Woyciechowski, Non-bee insects are important contributors to global crop pollination. *Proc. Natl. Acad. Sci.* **113**, 146–151 (2016).

10. A.-M. Klein, B. E. Vaissière, J. H. Cane, I. Steffan-Dewenter, S. A. Cunningham, C. Kremen, T. Tscharntke, Importance of pollinators in changing landscapes for world crops. *Proc. R. Soc. B Biol. Sci.* **274**, 303–313 (2007).

11. WHO, "Guidance on mainstreaming biodiversity for nutrition and health" (World Health Organization, Geneva, 2020).

12. O. Dangles, J. Casas, Ecosystem services provided by insects for achieving sustainable development goals. *Ecosyst. Serv.* **35**, 109–115 (2019).

13. F. L. W. Ratnieks, N. L. Carreck, Clarity on Honey Bee Collapse? *Science*. **327**, 152–153 (2010).

14. D. vanEngelsdorp, J. D. Evans, C. Saegerman, C. Mullin, E. Haubruge, B. K. Nguyen, M. Frazier, J. Frazier, D. Cox-Foster, Y. Chen, R. Underwood, D. R. Tarpy, J. S. Pettis, Colony Collapse Disorder: A Descriptive Study. *PLoS ONE*. **4**, e6481 (2009).

15. A. Gray, N. Adjlane, A. Arab, A. Ballis, V. Brusbardis, J.-D. Charrière, R. Chlebo, M. F. Coffey, B. Cornelissen, C. Amaro da Costa, B. Dahle, J. Danihlík, M. M. Dražić, G. Evans, M. Fedoriak, I. Forsythe, A. Gajda, D. C. de Graaf, A. Gregorc, I. Ilieva, J. Johannesen, L. Kauko, P. Kristiansen, M. Martikkala, R. Martín-Hernández, C. A. Medina-Flores, F. Mutinelli, S. Patalano, A. Raudmets, G. S. Martin, V. Soroker, J. Stevanovic, A. Uzunov, F. Vejsnaes, A. Williams, M. Zammit-Mangion, R. Brodschneider, Honey bee colony winter loss rates for 35 countries participating in the COLOSS survey for winter 2018–2019, and the effects of a new queen on the risk of colony winter loss. *J. Apic. Res.* **59**, 744–751 (2020).

16. N. Seitz, K. S. Traynor, N. Steinhauer, K. Rennich, M. E. Wilson, J. D. Ellis, R. Rose, D. R. Tarpy, R. R. Sagili, D. M. Caron, K. S. Delaplane, J. Rangel, K. Lee, K. Baylis, J. T. Wilkes, J. A. Skinner, J. S. Pettis, D. vanEngelsdorp, A national survey of managed honey bee 2014–2015 annual colony losses in the USA. *J. Apic. Res.* **54**, 292–304 (2015).

17. R. van der Zee, L. Pisa, S. Andonov, R. Brodschneider, J.-D. Charrière, R. Chlebo, M. F. Coffey, K. Crailsheim, B. Dahle, A. Gajda, A. Gray, M. M. Drazic, M. Higes, L. Kauko, A. Kence, M. Kence, N. Kezic, H. Kiprijanovska, J. Kralj, P. Kristiansen, R. M. Hernandez, F. Mutinelli, B. K. Nguyen, C. Otten, A. Özkırım, S. F. Pernal, M. Peterson, G. Ramsay, V. Santrac, V. Soroker, G. Topolska, A. Uzunov, F. Vejsnæs, S. Wei, S. Wilkins, Managed honey bee colony losses in Canada, China, Europe, Israel and Turkey, for the winters of 2008–9 and 2009–10. *J. Apic. Res.* **51**, 100–114 (2012).

18. T. D. Seeley, *The Wisdom of the Hive: the social physiology of honey bee colonies* (Harvard University Press, 1995).

19. M. A. Döke, M. Frazier, C. M. Grozinger, Overwintering honey bees: biology and management. *Curr. Opin. Insect Sci.* **10**, 185–193 (2015).

20. H. R. Mattila, J. L. Harris, G. W. Otis, Timing of production of winter bees in honey bee (Apis mellifera) colonies. *Insectes Sociaux*. **48**, 88–93 (2001).

21. J. Krause, A. F. T. Winfield, J.-L. Deneubourg, Interactive robots in experimental biology. *Trends Ecol. Evol.* **26**, 369–375 (2011).

22. G. L. Patricelli, "Use of Robotics in the Study of Animal Behavior" in *Encyclopedia of Animal Behavior (Second Edition)*, J. C. Choe, Ed. (Academic Press, Oxford, 2019), pp. 535–545.

23. D. Romano, E. Donati, G. Benelli, C. Stefanini, A review on animal–robot interaction: from bio-hybrid organisms to mixed societies. *Biol. Cybern.* **113**, 201–225 (2019).

24. T. Landgraf, G. H. W. Gebhardt, D. Bierbach, P. Romanczuk, L. Musiolek, V. V. Hafner, J. Krause, Animal-in-the-Loop: Using Interactive Robotic Conspecifics to Study Social Behavior in Animal Groups. *Annu. Rev. Control Robot. Auton. Syst.* **4**, 487–507 (2021).

25. S. Agrawal, S. Safarik, M. H. Dickinson, *J. Exp. Biol.*, in press, doi:10.1242/jeb.105817.

26. H. Ishii, M. Ogura, S. Kurisu, A. Komura, A. Takanishi, N. Iida, H. Kimura, "Experimental Study on Task Teaching to Real Rats Through Interaction with a Robotic Rat" in *From Animals to Animats 9*, S. Nolfi, G. Baldassarre, R. Calabretta, J. C. T. Hallam, D. Marocco, J.-A. Meyer, O. Miglino, D. Parisi, Eds. (Springer Berlin Heidelberg, Berlin, Heidelberg, 2006), vol. 4095 of *Lecture Notes in Computer Science*, pp. 643–654.

27. F. Patane, V. Mattoli, C. Laschi, B. Mazzolai, P. Dario, H. Ishii, A. Takanishi, "Biomechatronic Design and Development of a Legged Rat Robot" in *2007 IEEE International Conference on Robotics and Biomimetics (ROBIO)* (IEEE, Sanya, 2007), pp. 847–852.

28. R. Vaughan, N. Sumpter, J. Henderson, A. Frost, S. Cameron, Experiments in automatic flock control. *Robot. Auton. Syst.* **31**, 109–117 (2000).

29. D. T. Swain, I. D. Couzin, N. Ehrich Leonard, Real-Time Feedback-Controlled Robotic Fish for Behavioral Experiments With Fish Schools. *Proc. IEEE*. **100**, 150–163 (2012).

30. J. Halloy, G. Sempo, G. Caprari, C. Rivault, M. Asadpour, F. Tache, I. Said, V. Durier, S. Canonge, J. M. Ame, C. Detrain, N. Correll, A. Martinoli, F. Mondada, R. Siegwart, J. L. Deneubourg, Social Integration of Robots into Groups of Cockroaches to Control Self-Organized Choices. *Science*. **318**, 1155–1158 (2007).

31. F. Mondada, J. Halloy, A. Martinoli, N. Correll, A. Gribovskiy, G. Sempo, R. Siegwart, J.-L. Deneubourg, "A General Methodology for the Control of Mixed Natural-Artificial Societies" in *Handbook of Collective Robotics*, S. Kernbach, Ed. (Pan Stanford, 2013; http://www.crcnetbase.com/doi/10.1201/b14908-19), pp. 547–586.

32. L. T. Reaney, R. A. Sims, S. W. M. Sims, M. D. Jennions, P. R. Y. Backwell, Experiments with robots explain synchronized courtship in fiddler crabs. *Curr. Biol.* **18**, R62–R63 (2008).

33. S. Camazine, J.-L. Deneubourg, N. R. Franks, J. Sneyd, G. Theraula, E. Bonabeau, *Self-organization in Biological Systems* (Princeton University Press, 2003).

34. J. B. Free, Y. Spencer-Booth, Chill-Coma and Cold Death Temperatures of Apis Mellifera. *Entomol. Exp. Appl.* **3**, 222–230 (1960).

35. B. Heinrich, "Social thermoregulation" in *The hot-blooded insects: strategies and mechanisms of thermoregulation* (Springer-Verlag Berlin Heidelberg, Berlin, Heidelberg, 1993).

36. H. Esch, The Effects of Temperature on Flight Muscle Potentials in Honeybees and Cuculiinid Winter Moths. *J. Exp. Biol.* **135**, 109–117 (1988).

37. J. Lecomte, Sur le determinisme de la formation de la grappe chez les abeilles. *Z. Vgl. Physiol.* **32**, 499–506 (1950).

38. M. Szopek, T. Schmickl, R. Thenius, G. Radspieler, K. Crailsheim, Dynamics of Collective Decision Making of Honeybees in Complex Temperature Fields. *PLOS ONE*. **8**, e76250 (2013).

39. J. C. Jones, M. R. Myerscough, S. Graham, B. P. Oldroyd, Honey Bee Nest Thermoregulation: Diversity Promotes Stability. *Science*. **305**, 402–404 (2004).

40. B. Bujok, M. Kleinhenz, S. Fuchs, J. Tautz, Hot spots in the bee hive. *Naturwissenschaften*. **89**, 299–301 (2002).

41. S. Kühnholz, T. D. Seeley, The control of water collection in honey bee colonies. *Behav. Ecol. Sociobiol.* **41**, 407–422 (1997).

42. C. N. Cook, S. Durzi, K. J. Scheckel, M. D. Breed, Larvae influence thermoregulatory fanning behavior in honeybees (Apis mellifera L.). *Insectes Sociaux*. **63**, 271–278 (2016).

43. R. E. Bonoan, R. R. Goldman, P. Y. Wong, P. T. Starks, Vasculature of the hive: heat dissipation in the honey bee (Apis mellifera) hive. *Naturwissenschaften*. **101**, 459–465 (2014).

44. A. Stabentheiner, H. Pressl, T. Papst, N. Hrassnigg, K. Crailsheim, Endothermic heat production in honeybee winter clusters. *J. Exp. Biol.* **206**, 353–358 (2003).

45. E. E. Southwick, Metabolic energy of intact honey bee colonies. *Comp. Biochem. Physiol. A Physiol.* **71**, 277–281 (1982).

46. K. Griparic, T. Haus, D. Miklic, S. Bogdan, "Combined actuator sensor unit for interaction with honeybees" in *2015 IEEE Sensors Applications Symposium (SAS)* (IEEE, Zadar, Croatia, 2015), pp. 1–5.

47. M. Stefanec, M. Szopek, T. Schmickl, R. Mills, "Governing the swarm: Controlling a bio-hybrid society of bees robots with computational feedback loops" in *2017 IEEE Symposium Series on Computational Intelligence (SSCI)* (2017), pp. 1–8.

48. T. Schmickl, M. Szopek, F. Mondada, R. Mills, M. Stefanec, D. N. Hofstadler, D. Lazic, R. Barmak, F. Bonnet, P. Zahadat, Social Integrating Robots Suggest Mitigation Strategies for Ecosystem Decay. *Front. Bioeng. Biotechnol.* **9**, 612605 (2021).

49. C. D. Owens, *The Thermology of Wintering Honey Bee Colonies* (U.S. Agricultural Research Service, 1971).

50. E. E. Southwick, "Overwintering in Honey Bees: Implications for Apiculture" in *Insects at Low Temperature*, R. E. Lee, D. L. Denlinger, Eds. (Springer US, Boston, MA, 1991), pp. 446–460.

51. T. S. K. Johansson, M. P. Johansson, The Honeybee Colony in Winter. *Bee World*. **60**, 155–170 (1979).

52. B. Kraus, H. H. W. Velthuis, S. Tingek, Temperature profiles of the brood nests of Apis cerana and Apis mellifera colonies and their relation to varroosis. *J. Apic. Res.* **37**, 175–181 (1998).

53. D. Severson, E. Erickson Jr, Quantification of cluster size and low ambient temperature relationships in the honey bee. *Apidologie*. **21**, 135–142 (1990).

54. T. I. Szabo, The Thermology of Wintering Honeybee Colonies in 4-Colony Packs as Affected by Various Hive Entrances. *J. Apic. Res.* **24**, 27–37 (1985).

55. E. E. Southwick, G. Heldmaier, Temperature Control in Honey Bee Colonies. *BioScience*. **37**, 395–399 (1987).

56. J. R. Harbo, Effect of Population Size on Worker Survival and Honey Loss in Broodless Colonies of Honey Bees, Apis mellifera L. (Hymenoptera: Apidae) 1. *Environ. Entomol.* **12**, 1559–1563 (1983).

57. W. G. Meikle, N. Holst, Application of continuous monitoring of honeybee colonies. *Apidologie*. **46**, 10–22 (2015).

58. G. Retschnig, G. R. Williams, R. Odemer, J. Boltin, C. Di Poto, M. M. Mehmann, P. Retschnig, P. Winiger, P. Rosenkranz, P. Neumann, Effects, but no interactions, of ubiquitous pesticide and parasite stressors on honey bee (Apis mellifera) lifespan and behaviour in a colony environment. *Environ. Microbiol.* **17**, 4322–4331 (2015).

59. T. D. Seeley, "Temperature control" in *The Lives of Bees: The Untold Story of the Honey Bee in the Wild* (Princeton University Press, 2019).

60. E. Rademacher, M. Harz, S. Schneider, Effects of Oxalic Acid on Apis mellifera (Hymenoptera: Apidae). *Insects*. **8**, 84 (2017).

61. M. R. Myerscough, A Simple Model for Temperature Regulation in Honeybee Swarms. *J. Theor. Biol.* **162**, 381–393 (1993).

62. J. Watmough, S. Camazine, Self-Organized Thermoregulation of Honeybee Clusters. *J. Theor. Biol.* **176**, 391–402 (1995).

63. D. J. T. Sumpter, D. S. Broomhead, Shape and Dynamics of Thermoregulating Honey Bee Clusters. *J. Theor. Biol.* **204**, 1–14 (2000).

64. S. A. Ocko, L. Mahadevan, Collective thermoregulation in bee clusters. *J. R. Soc. Interface*. **11**, 20131033 (2014).

65. R. Bastiaansen, A. Doelman, F. van Langevelde, V. Rottschäfer, Modeling Honey Bee Colonies in Winter Using a Keller--Segel Model With a Sign-Changing Chemotactic Coefficient. *SIAM J. Appl. Math.* **80**, 839–863 (2020).

66. B. Heinrich, Energetics of Honeybee Swarm Thermoregulation. *Science*. **212**, 565–566 (1981).

67. A. Stabentheiner, H. Kovac, M. Mandl, H. Käfer, Coping with the cold and fighting the heat: thermal homeostasis of a superorganism, the honeybee colony. *J. Comp. Physiol. A* (2021), doi:10/gpw4t3.

68. I. Nolasco, A. Terenzi, S. Cecchi, S. Orcioni, H. L. Bear, E. Benetos, "Audio-based Identification of Beehive States" in *ICASSP 2019 - 2019 IEEE International Conference on Acoustics, Speech and Signal Processing (ICASSP)* (IEEE, Brighton, United Kingdom, 2019), pp. 8256–8260.

69. A. Szczurek, M. Maciejewska, B. Bąk, J. Wilde, M. Siuda, Semiconductor gas sensor as a detector of Varroa destructor infestation of honey bee colonies – Statistical evaluation. *Comput. Electron. Agric.* **162**, 405–411 (2019).

70. Y. Le Conte, G. Arnold, Ph. Desenfant, Influence of Brood Temperature and Hygrometry Variations on the Development of the Honey Bee EctoparasiteVarroa jacobsoni(Mesostigmata: Varroidae). *Environ. Entomol.* **19**, 1780–1785 (1990).

71. K. Bozek, L. Hebert, Y. Portugal, A. S. Mikheyev, G. J. Stephens, Markerless tracking of an entire honey bee colony. *Nat. Commun.* **12**, 1733 (2021).

72. D. Mitchell, Ratios of colony mass to thermal conductance of tree and man-made nest enclosures of Apis mellifera: implications for survival, clustering, humidity regulation and Varroa destructor. *Int. J. Biometeorol.* **60**, 629–638 (2016).

73. F. Kronenberg, H. C. Heller, Colonial thermoregulation in honey bees (Apis mellifera). *J. Comp. Physiol.* **148**, 65–76 (1982).

74. G. W. Otis, Weights of Worker Honeybees in Swarms. *J. Apic. Res.* **21**, 88–92 (1982).

75. E. E. Southwick, D. Pimentel, Energy Efficiency of Honey Production by Bees. *BioScience*. **31**, 730–732 (1981).

76. A. Ramdas, R. J. Tibshirani, Fast and flexible ADMM algorithms for trend filtering. *J. Comput. Graph. Stat.* **25**, 839–858 (2016).

77. R. J. Tibshirani, Adaptive piecewise polynomial estimation via trend filtering. *Ann. Stat.* **42**, 285–323 (2014).

78. B. Bruder, T.-L. Dao, J.-C. Richard, T. Roncalli, Trend Filtering Methods for Momentum Strategies. *SSRN Electron. J.* (2011), doi:10.2139/ssrn.2289097.

79. G. Farnebäck, "Two-Frame Motion Estimation Based on Polynomial Expansion" in *Image Analysis*, J. Bigun, T. Gustavsson, Eds. (Springer, Berlin, Heidelberg, 2003), *Lecture Notes in Computer Science*, pp. 363–370.

80. Z. Zivkovic, "Improved adaptive Gaussian mixture model for background subtraction" in *Proceedings of the 17th International Conference on Pattern Recognition, 2004. ICPR 2004.* (2004), vol. 2, pp. 28-31 Vol.2.

81. S. Suzuki, K. be, Topological structural analysis of digitized binary images by border following. *Comput. Vis. Graph. Image Process.* **30**, 32–46 (1985).

82. P. J. Rousseeuw, M. Hubert, Anomaly detection by robust statistics. *WIREs Data Min. Knowl. Discov.* **8**, e1236 (2018).

83. A. J. Ijspeert, Biorobotics: Using robots to emulate and investigate agile locomotion. *Science*. **346**, 196–203 (2014).

84. N. W. Xu, J. O. Dabiri, Low-power microelectronics embedded in live jellyfish enhance propulsion. *Sci. Adv.* **6**, eaaz3194 (2020).

85. T. T. Vo Doan, M. Y. W. Tan, X. H. Bui, H. Sato, An Ultralightweight and Living Legged Robot. *Soft Robot.* **5**, 17–23 (2018).

86. J. Donhauser, A. van Wynsberghe, A. Bearden, Steps Toward an Ethics of Environmental Robotics. *Philos. Technol.* **34**, 507–524 (2021).

87. D. Grémillet, W. Puech, V. Garçon, T. Boulinier, Y. L. Maho, Robots in Ecology: Welcome to the machine. *Open J. Ecol.* **2**, 49–57 (2012).

88. I. L. Mason, "Evolution of domesticated animals" in (Longman, London, 1984), pp. 403–415.

89. M. D. Meixner, C. Costa, P. Kryger, F. Hatjina, M. Bouga, E. Ivanova, R. Büchler, Conserving diversity and vitality for honey bee breeding. *J. Apic. Res.* **49**, 85–92 (2010).

90. D. W. Scott, *Multivariate Density Estimation: Theory, Practice, and Visualization* (John Wiley & Sons, New York, Chicester, 1992).

Acknowledgments:

We thank Daniel Burnier and Norbert Crot for their suggestions on mechanical and electronic design, and the Botanical Gardens at the University of Graz for hosting the honeybees.

Funding:

This work was supported by the EU H2020 FET project HIVEOPOLIS (nº. 824069) and by the Field of Excellence COLIBRI (Complexity of Life in basic Research and Innovation) at the University of Graz.

Author contributions:

Conceptualization: RB, MS, DH, FM, TS, RM
Data curation: RB, DH, RM
Methodology: RB, MS, DH, LP, SS, FM, TS, RM
Investigation: RB, MS, DH, TS, RM
Formal analysis: RB, MS, DH, RM
Visualization: RB, DH
Software: RB, DH, LP, RM
Writing – original draft: RB, MS, DH, TS, RM
Writing – review & editing: RB, MS, DH, LP, SS, FM, TS, RM

Competing interests: Authors declare that they have no competing interests.

Data and materials availability:

All (other) data needed to evaluate the conclusions in the paper are present in the paper or the Supplementary Materials. The data and the software for this study have been deposited in the Zenodo database at https://doi.org/10.5281/zenodo.7671163 (data) and https://doi.org/10.5281/zenodo.7671291 (software).

Science Robotics
AAAS

Supplementary Materials for

A robotic honeycomb for interaction with a honeybee colony

Rafael Barmak and Martin Stefanec, Daniel N. Hofstadler, Louis Piotet, Stefan Schönwetter-Fuchs-Schistek, Francesco Mondada, Thomas Schmickl, Rob Mills*

*Corresponding author. Email: rob.mills@epfl.ch

This PDF file includes:

Other Supplementary Materials for this manuscript include the following:

Movie S1 to S4

SUPPLEMENTARY METHODS

Method for estimating biohybrid energetic efficiency

Since energy consumption dictates the chances of surviving extended cold periods, we tried to estimate how much of the thermal energy, injected by the actuators, could have been exploited by the colony. We derived the estimation of energetic transfer as follows. For the duration of the modulating experiment, the robotic system activated pairs of thermal actuators operating at a median level of 1.54 W (=2 × 0.77 W). Both actuators injected a median daily energy of 120 kJ/day (or 6.13 MJ over 51 days). To estimate the energetic economy provided by the artificial agent, we must establish the energetic requirements of the living organism. A winter colony has metabolic heat production close to 20 W/kg at 10°C *(45)*, resulting in a steady metabolic expenditure of 10 W (=864 kJ/day) for a colony with a size similar to ours (4,000 individuals, weighing 0.5 kg). Assuming that all metabolic activity is supported by honey consumption and considering an energetic value of 12.72 MJ/kg for honey *(75)*, we project that the energy provided to the bees by the embedded robot is equivalent to a consumption of 68 g/day of honey. Thus, the actuators had the potential to provide up to 15% of the usual energetic demands of the colony's metabolic activity, if we assume that bees benefited from all the injected power (100% transfer efficiency). The levels of energy injected to modulate position were not dominant in terms of the colony's total energetic demand. Nonetheless, the bees were very responsive to the thermal signals, which points to their evolved capacities to collectively exploit available resources and hence increase their survival chances during cold periods.

Statistics and data analysis

Trend filtering

In some cases, where we had noisy time series (Figs. 3A, 5B), we used a modern denoising technique known as trend filtering *(76)* that tries to optimize the amount of noise reduction and data smoothing while maintaining the shape of the original signal *(77)*. The filtered signal is calculated by minimizing the following function,

$$\frac{1}{2}\sum_{t=1}^{n}\left(x_t - y_t\right)^2 + \lambda\left|D^{(k)}y_t\right|_1$$

where x_t is a scalar time series, y_t is the estimated trend, λ is a regularization parameter to trade-off denoise maximization (i.e., smoothness) and bias minimization (i.e., difference between observation and fitted values) *(78)*, and $D^{(k)}$ is the discrete difference operator of order k. We used λ=50 and order k=2.

Time series relationships

To quantify temporal similarities between two variables (e.g., between temperature series or the position of the bee cluster to actuators activation series), we performed a time-lagged nonparametric Spearman rank correlation. The correlation coefficient ρ_s, the values of peak synchrony lag, in hours or days, and the two-sided p-value of the significance test are reported.

Visual data sampling and processing

Cameras from both sides of the robotic device were triggered every four seconds and images with a resolution of 4056 × 3040 pixels were temporarily stored in the memory card of the SBC controlling the camera. Since photos suffered barrel distortions caused by the wide-angle lens, we calibrated one camera of the setup and the resulting correction matrix and coefficients were used, in post-processing, to undistort all collected images. To correct minor misalignment between cameras and comb centers, images were processed with a linear transformation to correct for perspective distortions. Finally, the global contrast of each image was increased by sharpening (via "unsharp masking") and performing histogram equalization.

To find how the winter cluster was thermally structured, we analyzed the collected images to identify the perimeter delimiting the core and the outer edge of the cluster that encompassed most bees. The core of the cluster is identified by the perimeter of the region with high bee motility, close to the center of the cluster *(49, 62)*, which implies that portions of the images with higher levels of pixel movement can provide a robust approximation of the cluster core. Hence, to detect the level of pixel movement, we computed the dense optical flow of two consecutive frames (Δt=4s) in intervals of 10 min using Farnebäck's algorithm *(79)*. We computed the magnitude of the optical flow vector field to find the contours of the regions with high pixel motility (i.e., high flow magnitude) and selected the biggest contour as the core representative region. From this contour, we extracted metrics including area, perimeter length, and centroid. To find the contour of the outer edge of the cluster, a background image of the honeycomb was first computed, using the Gaussian mixture-based background/foreground segmentation algorithm *(80)*, using one image per hour. Each image was scaled to 30% of the original size and then processed with a histogram equalizer and a Gaussian blur filter. The images were then thresholded depending on the brightness level of the background image: darker areas of the background image required a lower threshold to be counted as part of the cluster while lighter areas required a higher threshold. In total, three brightness zones were defined so that different brightness levels in the image were compensated. This resulted in a binary image in which erosion and dilation operations assisted in removing noise. The contour of the binary geometry was computed using a border-following algorithm *(81)*.

Thermal data analysis

Based on data from the 64 temperature sensors, we reconstructed the thermal field across the bee-occupied region of the robotic device using a linear interpolation method. We detected failures in two sensors (positions x,y = 3,3 and 5,1) from Colony A device and excluded the data produced by these from our analysis.

Combining thermal and visual data

To find the representative temperatures in the regions of the mantle and the core, we sampled the interpolated thermal fields at the points contained by the perimeter curves calculated from optical data. We segmented each computed contour into 100 equidistant points, obtained temperature values for each one from the thermal fields, and then reduced to one value, calculated by the median and the uncertainty by the MAD. This process was repeated for each timestep, forming the temporal evolution of the temperature in the core center, core periphery, and mantle contour (see Fig. 3A). Finally, the median of each temporal series and the median of its uncertainties

(MADs) were used to find a single representative value for those regions ($\overline{T}_{mantle}$, $\overline{T}_{core}$, and $\overline{T}_{cen}$, see Fig. 3C).

Modulation experiment metrics

During the modulation experiment, the position and the size of the cluster were estimated in intervals of 30 minutes, using the previously described adaptive background subtraction method, resulting in n=2,448 estimates for the back and front sub-clusters. To analyze the cluster response to each new actuator activation, we investigated the commonalities of n=32 activations, each lasting 3 days. Once a new pair of actuators was turned on, we calculate the temporal evolution of the absolute distance between the active actuator center and the cluster centroid, $d = |x_{actuator} - x_{cluster}|$. Each 3-day activation resulted in 144 distances,

$$d_t^1 = \left\{ d_0^1, \ldots, d_{t=144}^1 \right\}$$
$$\ldots$$
$$d_t^{32} = \left\{ d_0^{32}, \ldots, d_{t=144}^{32} \right\}$$

Then, the median movement, from the 32 distance vectors, was calculated by the median of all distances at each time step, $d = \{med(d_0^1,\ldots, d_0^{32}),\ldots, med(d_{144}^1,\ldots, d_{144}^{32})\}$. The uncertainty of the distance measurements is given by the robust estimator of scale MAD, calculated by the median of all absolute distances from the sample median *(82)*:
$MAD_t = 1.483 \cdot median_{j=1\ldots N}\left|d_t^j - median_{i=1\ldots N} d_t^i\right|$, resulting in a vector with one MAD value for each time step, MAD = {MAD_0, MAD_1, …, MAD_{t-1}, MAD_t}. The results of this analysis can be seen in Fig. S1.

SUPPLEMENTARY DISCUSSION

Ethical considerations for using the robotic honeycomb

Unlike biorobotics, where biology is a source of inspiration for creating new biomimetic devices (such as *(83)*), interactive robotic systems presuppose proximity and information exchange with living animals *(21–23, 31)*. Although not as invasive as cyborgs, where sometimes electrodes are surgically implanted into the animal (*84, 85*), the creation of mixed societies, where animals are exposed to artificial agents, is not necessarily free of unintended and lasting consequences for individual animals (i), colonies (ii), or their habitats (iii) *(86, 87)*. Our results demonstrate that robotics can be used for extended periods embedded in a colony. So, what are the ethical considerations of such systems? In *(48)*, we explored some of the ethical considerations we followed in designing our robotic systems and conducting experiments. For instance, to address potential unintended consequences on the individual level (i), we restricted the interaction pathway between the artificial agent and bees to thermal stimuli with intensities normally encountered in honeybee thermoregulatory behaviors to minimize stress. When moving outside of the hive, honeybees interact with their ecosystem (iii), for example, by foraging. However, due to the technology being confined to the hive, any negative effects at the ecosystem level are expected to be similar to those that a strong, robust honeybee colony would have without being augmented by the technology. Lastly, the potential effects on the colony, and more broadly, the species, should be taken into account (ii). The honeybees we used are managed livestock and like other domesticated species, natural selection no longer shapes their evolution *(88, 89)*. Instead, artificial selection by bee breeders has favored traits such as tameness and high honey yield. If a robotic system were to assist a weak colony in surviving, the colony might eventually reproduce through swarming. Any resulting feral daughter colony would lack access to supportive robotics, and its weaknesses would be exposed to natural selection. This greatly limits the potential for our robotic systems to have a lasting effect on the evolution of feral honeybees.

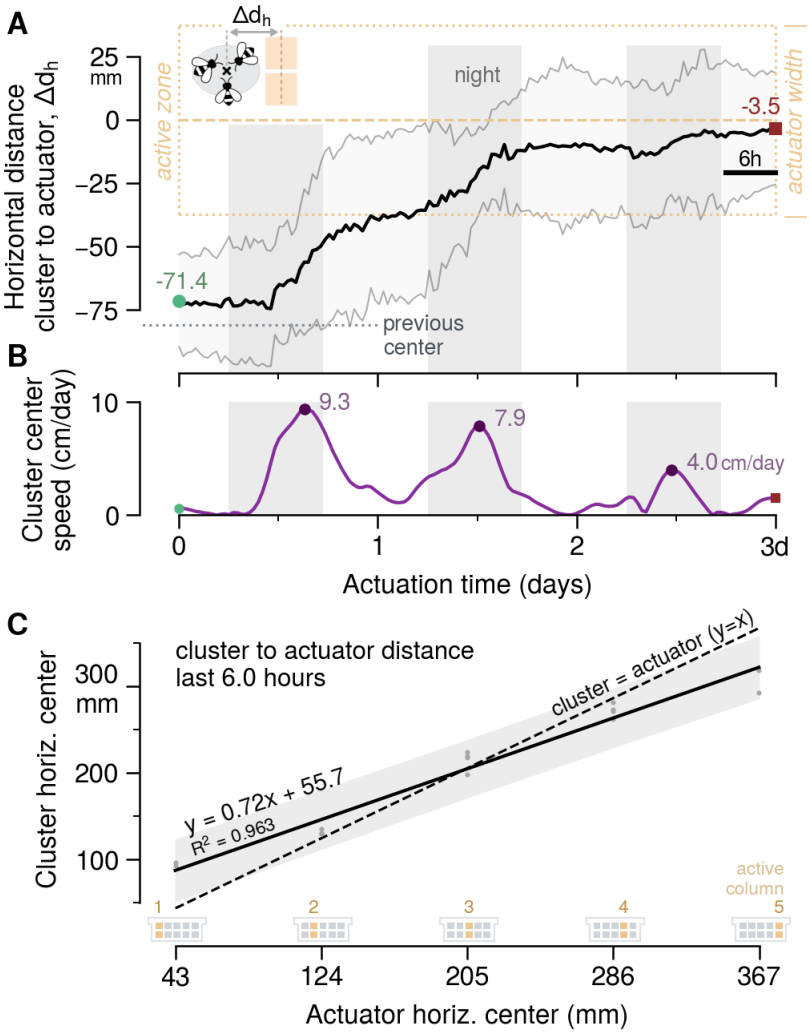

Fig. S1. Dynamics of cluster motion towards thermal stimuli. (**A**) Movement of the cluster's horizontal center towards the center of an active actuator. The black curve is the median value of n=32 cluster movements towards newly heated zones Δd_h (from back and front sub-clusters). Each zone, spanning two actuators, was active for 3 days. The uncertainty of the distance Δd_h is calculated by the MAD and represented by the region delimited by the two thin gray lines. Active actuators' horizontal boundaries are depicted by the dotted yellow lines, with the dashed yellow line indicating the horizontal center. The green and red markers indicate the initial and final distances from the cluster centroid to the new actuator center. The vertical gray bands depict astronomical nights. (**B**) Median cluster horizontal speed smoothed by a trend filter (purple). (**C**) Linear least-squares regression depicting the influence of the active actuators in the final position of the winter cluster. The gray dots are Δd_h from the last 6h of each activation window (n=16 median distances). The gray zone represents the 95% sample confidence interval. The dashed line shows a hypothetical cluster centroid aligned with the active zone's center. The analysis of these metrics is described above in "Modulation experiment metrics".

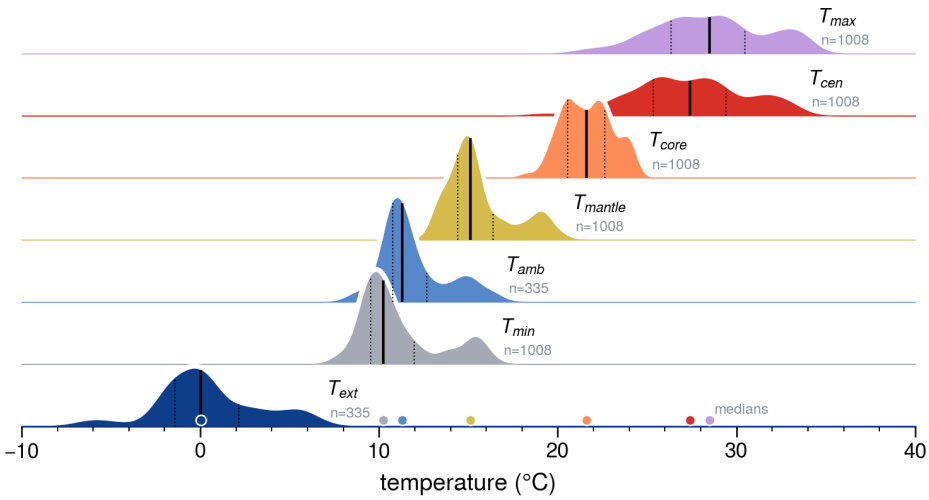

Fig. S2. Data distributions for the observation experiment. Probability density functions (PDF) computed through a nonparametric kernel density estimator (KDE) for each temperature series in Fig. 3. The Gaussian kernel size was automatically defined via Scott's method *(90)*. On each distribution, the thick black line indicates the median value, and the thin lines the 25 and 75 percentiles.

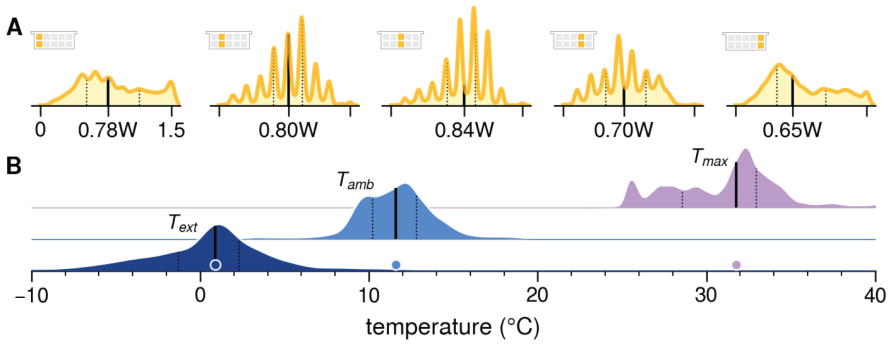

Fig. S3. Data distributions for collective position modulation experiment. (**A**) Dissipated power PDFs for each active actuator's column during the 51 days of the experiment. (**B**) PDFs of relevant temperatures during the modulation experiment. As in the previous figure, the thick black line indicates the median and the thin lines the 25 and 75 percentiles. The distributions are related to the series depicted in Fig. 5.

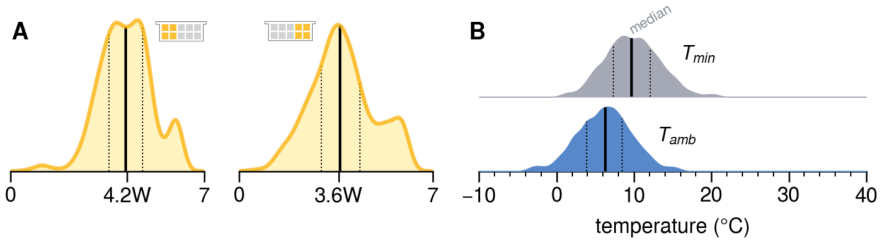

Fig. S4. Data distributions for the autonomous closed-loop experiment. (**A**) Dissipated power PDFs for active periods of the left and right attraction, comprising 4 actuators each, during the 17 days of the experiment. (**B**) PDFs of relevant temperatures during the closed-loop experiment. The distributions are related to the series depicted in Fig. 7.

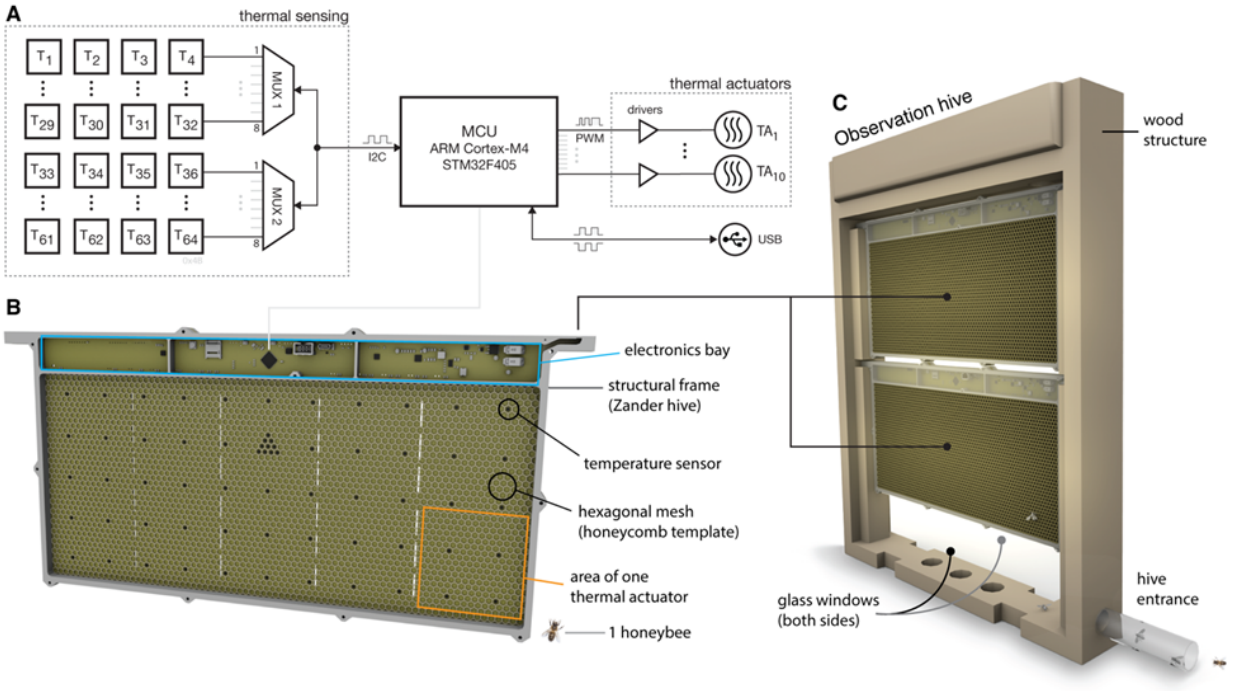

Fig. S5. Structure and design of the robotic honeybee comb. (**A**) Functional architecture, comprising arrays of thermal sensors and actuators, and a microcontroller as the orchestrator of the system. (**B**) 3D render with indications to main system component positions. (**C**) 3D diagram of the double-frame observation hives used in this study. Non-reflective glass on each side of the hive allowed visual data to be collected whilst maintaining an enclosed volume for the colony. Bees had unrestricted access to the exterior by a pipe connecting a perforation in the HFLG's wall and the hive entrance.

Legends for Supporting Movies

Movie S1. Time-lapse of the observation experiment showing pictures and thermal profiles of the winter cluster.

Movie S2. Time-lapse showing modulation of the winter cluster's position.

Movie S3. Annotated video depicting the evolution of a winter cluster, from the formation of a cluster until the "resuscitation" effort after the collapse of the colony.

Movie S4. Autonomous closed-loop collective position modulation experiment depicting visual, thermal, and robot-processed data.

Legends for Data Files

Data file 1. Original thermal data in the observation result.

Data file 2. Original thermal data in the position modulation result.

Data file 3. Original thermal data in the autonomous closed-loop result.

Data file 4. Original thermal data in the colony collapse results.